The Mesozoic palaeorelief of the northern Tian Shan (China)

Ke Chen, Charles Gumiaux, Romain Augier, Yan Chen, Qingchen Wang, Wei Lin, Shengli Wang

The Mesozoic palaeorelief of the northern Tian Shan (China)

Ke CHEN[1,2], Charles GUMIAUX[1], Romain AUGIER[1], Yan CHEN[1], Qingchen WANG[2] , Wei LIN[2] , Shengli WANG[3] ,

1. Institut des Sciences de la Terre d'Orléans (ISTO), Université d'Orléans, CNRS: UMR6113, Université François Rabelais - Tours, - INSU, Campus Géosciences, 1A rue de la Férollerie, 45071 Orléans cedex 2, France

2. State Key Laboratory of Lithospheric Evolution, Institute of Geology and Geophysics, Chinese Academy of Sciences, P.O. 9825, Beijing 100029, China

3. Department of Earth Sciences, Nanjing University, 210093, Nanjing, China

Abstract

The Tian Shan range offers a natural laboratory to study orogenic processes. Most of the previous studies focused on either the Paleozoic evolution of the range or its Cenozoic intracontinental evolution linked with the India-Asia collision. In this study, detailed field investigations on the relationship between sedimentary cover and basement constrain the Mesozoic evolution of the northern Tian Shan. Sedimentological observations argue for limited transport distance for Lower and Uppermost Jurassic deposits. Geological sections presented in this paper show that, in preserved locations, Triassic to Jurassic sedimentary series present a continuous onlap type sedimentary unconformity on the top of the basement. At different scales, observations clearly evidence the existence of a major palaeorelief during Mesozoic. According to the present study, the current Tian Shan range topography and the associated movements along its northern front structures cannot be considered as the consequence of Cenozoic reactivation alone.

Keywords

Tian Shan, palaeorelief, Mesozoic, regional onlap, reactivation, India-Asia collision.

Introduction

The modern Tian Shan is one of the major mountain ranges in Central Asia. The current structure of Tian Shan mainly results from a combination of two main tectonic events: i) subductions, arc-accretions and continental collision during Paleozoic (e.g. Carroll et al., 1990; Wang et al., 1990; Windley et al., 1990; Sengör et al. 1993; Carroll et al., 1995; Gao et al., 1998; Laurent-Charvet et al., 2002; Charvet et al., 2007; Wang et al., 2007) and ii) intracontinental reactivation linked to the India-Asia collision, during Cenozoic (e.g. Tapponnier and Molnar, 1977; Avouac et al., 1993). At first order, the modern Tian Shan corresponds to a raised ~east-west trending Paleozoic 'basement' range, flanked by two closed intracontinental basins whose infill is a particularly accurate record for both tectonic and climate evolutions (Fig. 1). The present-day high topography of Tian Shan, with a mean altitude of ~2500 m and summits of more than 7000 m, is traditionally related to the latest intracontinental deformation of the range (e.g. Tapponnier and Molnar, 1977; Avouac et al., 1993; Burchfiel et al., 1999). Age constraints for the onset of this intracontinental reactivation range from 10 to 24 Ma (e.g. Avouac et al., 1993; Hendrix et al., 1994; Abdrakhmatov et al., 1996; Métivier and Gaudemer, 1997; Sobel et al., 1997; Dumitru et al., 2001; Charreau et al., 2009). In spite of relative age discrepancies (mostly related to the method applied), all ages estimated for the deformation and the associated relief erosion suggest that the mountain range reactivation and relief creation began during Early Miocene at oldest.

However, recent Fission-track analyses suggest that uplifting may have existed well before the onset of the Tertiary reactivation through Tian Shan, with exhumation ages such as 160-120 Ma in central Tian Shan, 200-250 Ma detritus cooling age in the Manas River valley (Dumitru et al., 2001; Jolivet et al., 2010) or 140-120 Ma from Bayanbulak intracontinental basin, in the southern Tian Shan (Wang et al., 2009). Moreover, Triassic to Cretaceous sediments are composed of thick continental series characterized by massive coarse-grained

formations within both basins, suggesting rather high erosion rate at that time (Hendrix, 2000; Carroll et al., 2010).

This study considers the Mesozoic tectonic and morphologic evolution of Tian Shan through field structural and sedimentological analyses of Mesozoic deposits. It focuses on the northern piedmont of the range, along a ~280 km west-east trending segment (Fig. 1). Thanks to deep incisions of seasonal rivers, contacts between Paleozoic basement and Mesozoic-Cenozoic sedimentary cover are particularly well exposed along several north-south trending sections in this region (Fig. 1). Such new constraints on Mesozoic evolution of the Tian Shan area would lead to reconsider the contribution of Cenozoic tectonics in the modern mountain range building as well as to better quantify the net shortening amount during that period.

Stratigraphy of the Mesozoic sediments within the study area

Sedimentary series can be extensively observed and have already been studied within the Junggar basin, as summarized below (Figs. 1 and 2; Hendrix et al., 1992 and references therein; XBGMR, 1993). Basement units of the north Tian Shan mainly consist of Paleozoic volcanic and sedimentary rocks. From bottom to top, the entire Mesozoic series is composed of ~5 km thick continental clastic deposits highlighting high sedimentation/preservation rates (Fig. 2). Thanks to numerous studies aimed at oil and gas exploration and to 1:200.000 mapping projects hold in this area, ages of the Mesozoic sequences were mainly constrained by floral and sporopollen assemblage analyses (Li et al., 1978; Yang et al., 1982; Liu, 1990; XBGMR, 1993; Lu and Deng, 2005; Yang et al., 2005; Huang and Li, 2007). In the study area, the Triassic series are mostly missing along the piedmont though locally exposed (Fig. 1). Where it crops out, Triassic displays alluvial sandstones and conglomerates intercalated within and silty mudstones (red-beds). At the scale of the northern Tian Shan piedmont, Lowermost Jurassic layers indicate a change in the sedimentation as they consist in thick and

coarse conglomeratic deposits, as exposed in the south of Qingshui He (Fig. 3a). Thickness of Lower Jurassic reaches 1000 m over the area extending from Manasi to Urumqi, and decreases westwardly and eastwardly. Sediments become progressively finer upward, grading into ~3 km thick series of Lower/Middle Jurassic gray sandstones, silty shales (Fig. 2). Middle Jurassic sandstones and mudstones locally contain coal-rich layers consistent with a lacustrine depositional facies (Hendrix et al., 1992). Upper Jurassic comprises typical fine-grained red beds where conglomerates remain scarce. The transition from Jurassic to Cretaceous series is marked by up to 800 m thick sedimentary breccias (Kalaza formation – J3k; Fig. 3b) made of coarse-grained angular clasts (Fig. 3c). It rapidly dies laterally and grades to sandstones within the Junggar basin itself (XBGMR, 1978; 1993). The marked unconformity between the Kalaza formation and the underlying finer-grained Upper Jurassic red beds (Fig. 3b) suggests a short transport distance of material before deposition and nearby relief uplifting.

In this study, Mesozoic sediments have also been extensively observed within internal parts of the range, and more particularly in the eastern part of the studied area (Fig. 1). Triassic to Jurassic sediments are encountered on top of the Paleozoic basement units, at rather high altitudes (2000 to 3000 m) in comparison with the mean altitude of the foreland fold-and-thrust belts (1000 to 1500 m high). In the Houxia valley for instance – 65 km SSW of Urumqi – a Lower to Upper Jurassic continuous sedimentary series is preserved in a syncline structure (Fig. 4a). According to the geological map (Fig. 4a; XBGMR, 1977), Lower Jurassic formations – i.e. Shangonghe Fm. to the northwest and Lowermost Jurassic Badaowan Fm. to the east – directly overlie on top of Carboniferous basement units, without intercalated Triassic sediments. Besides, south and north verging thrusts developed along parts of the northern and southern limbs of the fold, respectively (Fig. 4a). A section made across the north limb of the syncline displays continuous Lower to Middle Jurassic series with

no fault contact observed (Fig. 4b). From south to north, bedding planes progressively straighten up from ~30° south dipping to vertical, and even overturned just below the south verging thrust (Figs. 4a ,4b and 4d). From a sedimentological point of view, the upper and main part of Jurassic series is made of fine-grained sandstones and mudstones while the lowermost deposits of the series is characterized by intercalations of coarse-grained sedimentary breccias mostly made of highly angular clasts of Carboniferous tuffaceous sandstones (Fig. 4c). Local abundance of these breccias and the common lithological nature of the clasts with the adjacent basement unit strongly suggest a very short transport distance.

Structural analysis of the Mesozoic basal contact

Deformation of the northern Tian Shan has already been studied through the structural analysis of sedimentary series, within the Cenozoic foreland basin (e.g. Avouac et al., 1993; Deng et al., 1996; Burchfiel et al., 1999). This part focuses on the basal contact of the Mesozoic sediments, in the northern "front" area of Tian Shan.

As shown on the map (Fig. 1), some parts of the piedmont display northward thrusts that mark out the boundary in between the Paleozoic uplifted basement units and relatively subsiding proximal foreland basin. Yet, as described above, Mesozoic series are not solely restricted to the piedmont fold-and-thrust belts but are also well preserved on top of the basement units, within the range (Fig. 1). Then, some other segments of the piedmont display perfectly continuous Mesozoic sedimentary series from basin until internal and higher parts of the range, without being strained by any faulting or folding in the range front area (Fig. 1). Structural analysis of such unstrained basal contact of Mesozoic series is presented for two of the sections constructed from field work combined with available seismic profiles and drill-holes data: the Hutubi He and the Wusu sections (Fig. 1).

At first order, to the north of the Hutubi He area, Triassic to Neogene sedimentary series form a rather simple monocline structure, dipping 15-20° to the north (Fig. 5a). The southernmost fold-and-thrust belt is composed of one gentle upright anticline and associated syncline with only very limited thrusts developed along the hinge of the fold (Fig. 5a). This belt can be regarded as a fault-propagation fold structure according to the available seismic profile (Wang et al., 2005; Fig. 5b). Further south, entering within the interior parts of the range, sub-horizontal Lower Jurassic strata lie on top of the Carboniferous units (Fig. 5b). While basement is strongly deformed, as evidenced by sub-vertical cleavage, its sedimentary cover is only gently folded as illustrated on the geological map, few kilometers west of the river (Fig. 5a; XBGMR, 1978, 1993). No décollement structure has been observed between the basement top and the sedimentary cover. Besides, a southward backthrust of basement rocks above sediments can be observed to the south of the section, but the net slip must be limited as it rapidly dies out, the fault laterally evolving to a fold toward the west (Fig. 5a). Unconformity of the basal contact of Mesozoic sediments on top of basement units is observed in the southernmost part of the section (Figs. 5a and 6a). As a whole, the successive sub-horizontal and monocline segments define a hinge fold at regional scale (Fig. 5b). Nevertheless, while ~900 m thick of Triassic sediments have been drilled along the W1 well in the basin (Fig. 5b), no Triassic series have been observed further south in the range, in the section area (Fig. 5a). Indeed, Lowermost to Middle Jurassic levels have been observed and mapped directly on top of the basement units (Fig. 5a; XBGMR, 1978, 1993). Similarly to the Houxia area, basal contact of the Mesozoic series suggests its onlap deposit, from basin to range, at least during Triassic and Lower-Middle Jurassic.

More local-scale evidences for onlap sedimentation can also be observed in the Hutubi He area. First, to the south end of the section, Lower Jurassic strata display a kilometer scale onlap type structure on top of basement units, i.e. with younger sediments progressively

covering basement, from north to south (Figs. 5a and 6a). Second, ~10 km west of the Hutubi River, subhorizontal layers of the Lower Jurassic formation, which can be continuously followed in few kilometers in this small valley, structurally onlap on the deformed Paleozoic basement units (Fig. 6b). There, stratification planes are markedly oblique with the top of the Paleozoic units and no deformation has been observed along this contact. In the landscape, younger Jurassic sediments progressively extend to the south, on top of the Carboniferous units. Sediments progressively overlie and cover a ~150 m high step of the basement top which implies that a significant relief existed during Jurassic sediments deposition.

To the north of the Wusu section, first-order structure of the Mesozoic-Cenozoic series displays a 40-45° north dipping monocline (Figs. 7a and 7b). To the south, bedding is sub-horizontal and structure of the sedimentary series is marked by a large hinge fold. As drawn on the geological map, thrust faults are observed at the surface, but seismic data show that they do not extend downward into the Mesozoic series (Fig. 7b; *suppl. material*), which is compatible with the limited throw produced by these faults as deduced from map data analysis (Fig. 7a). While ~400 m of Triassic sediments have been found in a drilled well in the basin, close to this section (see W2 on Fig. 7a), Triassic series becomes much thinner to the south and Jurassic sandstones, sometimes, directly lie on top of the Carboniferous rocks with an erosional undeformed contact (Fig. 7c; XBGMR, 1973).

Discussion and conclusions

In parallel to rather classical view of frontal thrust systems, this study highlights that the northern piedmont of Tian Shan also displays segments where Mesozoic series are preserved unconformably onto the basement with onlap-type relationships. Such features are pointed out along two distant cross-sections and have also been clearly shown at outcrop-scale. Sedimentary breccias, showing very limited transport distances, have been found within

Lower Jurassic sediments of the internal parts of the range. Whatever the scale, all these observations clearly show the existence of proximal relief when Triassic/Jurassic sediments were deposited. Our field observations are consistent with previously published sedimentological data – paleocurrent measurements, heavy mineral composition, sedimentological source analyses – in the Junggar and Tarim basins which suggest that Tian Shan could already have existed as a "positive" geomorphologic feature during Mesozoic times (Hendrix et al., 1992, Graham et al., 1993; Hendrix, 2000; Li et al., 2004).

In the field, the local-scale observation of onlap sedimentary architecture reveals that the paleo-altitude difference can reach 100-150 m in a hectometer horizontal distance, which highlights local steep slopes (cf. Fig. 6b). Together with the sedimentological observations in the Houxia valley, this suggests that small-scale ridges with intercalated intra-mountainous basins have probably existed during Mesozoic (Fig. 8a).

Drill wells W1 and W1' (Figs. 4a and 4b) display ~1200 m of Lower Jurassic sediments (e.g. Badaowan and Shangonghe Fm., Fig. 2). A comparable thickness for Lower Jurassic has also been observed in the Manas area, 50 km west of the Hutubi section (Fig. 2; Hendrix et al., 1992). Following the geological maps (XBGMR; 1978, 1993), Middle Jurassic series directly lie unconformably onto the Carboniferous basement, without Triassic and Lower Jurassic sediments in the southern part of the Hutubi River (see location A in Fig. 4a). The thickness difference of Jurassic sediments reaches ~1200 m between the location A and the drill well location, for a horizontal distance of about 50 km (Fig. 4a). Such thickness difference may result from subsidence mechanisms. However, whatever the scale considered in this study, Triassic and mostly Jurassic series, up to the late Jurassic Kalaza formation deposit, display parallel bedding with no growth strata observed (Figs. 5b, 6 and 7b). Such feature shows that, at the scale of the studied area, significant vertical differential movements may have hardly occurred during Triassic to Upper Jurassic sedimentation. In addition, as

described above, Jurassic strata often overlie directly on Carboniferous by onlap, without fault or syn-sedimentary deformations. Seismic profiles across the southern margin of the Junggar basin do not display major fault that could have controlled sedimentation for the Early Jurassic period (Allen et al., 1991; Wang et al., 2005). No evidence for structural control on local subsidence could thus be argued here. At larger scale, flexure – either thermal or tectonic – could also have controlled the subsidence for Mesozoic series accumulation.

If considering thermal control, the latest regional tectono-magmatic event occurring before Mesozoic in the Central Tian Shan area ended during early Permian (see compilation by Han et al., 1999), which is about 100 Ma earlier than Jurassic sedimentation. Therefore, according to Hendrix et al. (1992), it seems that thermal driving mechanism may only play a weak role for the Early and Middle Jurassic sedimentation. If considering tectonic control, compressional flexure may also be hard to explain as, for comparable vertical differential movements, buckling of a stable continental lithosphere would result in much larger wavelength (200-300 km) than observed in this study (~50 km) as shown by mechanical modelling (Martinod and Davy, 1992, 1994; Burov et al., 1993; Cloetingh et al., 1999).

At the scale of the present study, Jurassic sedimentation seems hardly controlled by either tectonic or thermal subsidence across northern Tian Shan. Accordingly, the 1200-1300 m thickness difference may be mainly produced by infilling of a long-lasting remnant relief of, at least, 1200-1300 m high at that period (i.e. from Triassic/Lowermost Jurassic; Fig. 8a). During Middle Jurassic, finer-grained sediments were conformably deposited on top of the Lower Jurassic strata within the basin, and were deposited onlap on the Paleozoic basement toward the range (Figs. 5a and 8b). Middle Jurassic sediments of the Xishanyao and Toutunhe formations extend to a larger area with respect to the Lower Jurassic and, as a whole, the paleorelief lateral extension was certainly less important during Middle Jurassic than during Triassic/Early Jurassic (Fig. 8b). During latest Jurassic to Early Cretaceous, thick

breccias were deposited onto the Middle Jurassic sediments through an angular unconformity (*cf.* Kalaza Fm.). These breccias are restricted to the front of the modern Tian Shan and change rapidly to finer-grained deposits in lateral equivalents. This configuration is reminiscent of the general architecture of current fans deposited along the modern Tian Shan range that originate from the present day high relief to the south, but show limited northward transport of sediments (Fig. 8c). In turn, location of the main morphological northern front of the paleo- Tian Shan, during Latest Jurassic to Early Cretaceous, would approximately coincide with the one of the current range front (Fig. 5). The uplift documented by these coarse-grained sedimentary breccias is also recorded by AFT chronology studies; Fission-track modeling indicates a ca. 160 and 120 Ma cooling age along a Dushanzi-Kuqa corridor, in the mountain interior (Dumitru et al., 2001; Jolivet et al., 2010). Apatite sampled from Bayanbulak area yields the earliest cooling ages of Early Cretaceous (Dumitru et al., 2001; Wang et al. 2009).

Because no major tectonic event occurred in the Northern Tian Shan during Mesozoic times (e.g. De Grave et al., 2007), the Paleozoic subduction-collision orogeny (Gao et al., 1998; Laurent-Charvet et al., 2002; Charvet et al., 2007) appears as the most probable origin of the Mesozoic paleorelief above described. In such case, the Tian Shan would persist as remnant relieves for several tens of Ma after the end of the orogenic events which are progressively and unconformably overlain by Triassic and then Jurassic sedimentation (e.g. onlap structures, mesoscale paleorelief infilling). This scenario implies extremely low erosion rates to allow the preservation of a significant relief; such feature has already been reported for other regions of Central Asia from thermochronological (AFT) and field data analyses (Jolivet et al., 2007). In parallel, Central Asia Mesozoic tectonic history is marked by the polyphased Cimmerian orogeny in Tibet area (e.g. Hendrix et al., 1992; Sobel and Dumitru, 1997; De Grave et al., 2007). Low amplitude, far-field effects can thus be recognized in the

Mesozoic northern Tian Shan: one early collision stage – Qiantang/Kunlun blocks during Late Triassic/Middle Jurassic – would correspond to the drastic coarsening of the Lower Jurassic sedimentation. In turn, a later collision stage – Lhasa/Qiantang blocks during Late Jurassic/Early Cretaceous – well corresponds to the deposits of the thick and coarse breccias of the Kalaza Fm. at that time. In this case, a tectonic origin of the relief rejuvenation is attested by a major angular unconformity observed regionally.

As unambiguously demonstrated, the physiography of the modern Tian Shan dominantly results from the recent tectonic evolution of the area (e.g. Tapponnier and Molnar, 1977; Avouac et al., 1993; Métivier and Gaudemer, 1997; Charreau et al., 2009). However, this study put forward that the current Tian Shan topography can probably not be considered as the consequence of the Cenozoic intracontinental reactivation alone, but as a combination of the Cenozoic deformations superimposed on a reminiscent Mesozoic paleo-range. These new results question on the amplitude of the movements that could be estimated along the northern front structures during Cenozoic intracontinental reactivation.

Acknowledgements

Field and laboratory work in the present study are financially supported by Chinese National 973 Program (2009CB825008) and Chinese National S&T Major Project 2011ZX05008.

Prof. A.R. Caroll, Dr. J. Charreau, and an anonymous reviewer are warmly thanked for their constructive reviews. We are also grateful for the help by Prof. Carlo Doglioni (*Editor*) and Prof. Gerhard Wörner (*Associate Editor*). Discussions on seismic profiles' interpretation with Dr. Y. Branquet have also been greatly appreciated. The first author benefices a Ph.D scholarship from French Embassy in Beijing and IGGCAS.

References

Abdrakhmatov, K.Y., Aldazhanov, S.A., Hager, B.H., Hamburger, M.W., Herring, T.A., Kalabaev, K.B., Makarov, V.I., Molnar, P., Panasyuk, S.V., Prilepin, M.T., Reilinger, R.E., Sadybakasov, I.S., Souter, B.J., Trapeznikov, Y.A., Tsurkov, V.Y. and Zubovich, A.V., 1996. Relatively recent construction of the Tien Shan inferred from GPS measurements of present-day crustal deformation rates. *Nature*, **384**, 450-453.

Allen, M.B., Windley, B.F., Zhang, C., Zhao, Z.Y. and Wang, G.R., 1991. Basin Evolution within and Adjacent to the Tien-Shan Range, NW China. *J. Geol. Soc. London*, **148**, 369-378.

Avouac, J.P., Tapponnier, P., Bai, M., You, H. and Wang, G., 1993. Active Thrusting and Folding Along the Northern Tien-Shan and Late Cenozoic Rotation of the Tarim Relative to Dzungaria and Kazakhstan. *J. Geophys. Res.*, **98**, 6755-6804.

Burchfiel, B.C., Brown, E.T., Deng, Q.D., Feng, X.Y., Li, J., Molnar, P., Shi, J.B., Wu, Z.M. and You, H.C., 1999. Crustal shortening on the margins of the Tien Shan, Xinjiang, China. *Int. Geol. Rev.*, **41**, 665-700.

Burov, E.B., Lobkovsky, L.I., Cloetingh, S. and Nikishin, A.M., 1993. Continental lithosphere folding in Central Asia (Part II): constraints from gravity and topography. *Tectonophysics*, **226**, 73–87.

Carroll, A.R., Liang, Y., Graham, S.A., Xiao, X., Hendrix, M.S., Chu, J., and McKnight, C.L., 1990. Junggar basin, northwest China: Trapped late Paleozoic ocean. *Tectonophysics*, **181**, 1-14.

Carroll, A. R., Graham, S.A., Hendrix, M.S., Ying, D., and Zhou, D., 1995. Late Paleozoic tectonic amalgamation of northwestern China: sedimentary record of the northern Tarim, northwestern Turpan, and southern Junggar basins. *Geol. Soc. Am. Bull.*, **107**, 571-594.

Carroll, A.R., Graham, S.A. and Smith, M.E., 2010. Walled sedimentary basins of China. *Basin Res.*, **22**, 17-32.

Charreau, J., Chen, Y., Gilder, S., Barrier, L., Dominguez, S., Augier, R., Sen, S., Avouac, J.P., Gallaud, A., Graveleau, F. and Wang, Q.C., 2009. Neogene uplift of the Tian Shan Mountains observed in the magnetic record of the Jingou River section (northwest China). *Tectonics*, **28**, TC2008, doi:10.1029/2007TC002137.

Charvet, J., Shu, L.S. and Laurent-Charvet, S., 2007. Paleozoic structural and geodynamic evolution of eastern Tianshan (NW China): welding of the Tarim and Junggar plates. *Episodes*, **30**, 162-186.

Cloetingh, S., Burov, E. and Poliakov, A., 1999. Lithosphere folding: primary response to compression? (from central Asia to Paris basin). *Tectonics*, **18**, 1064–1083.

De Grave, J., Buslov, M.M. and Van den Haute, P., 2007. Distant effects of India–Eurasia convergence and Mesozoic intracontinental deformation in Central Asia: Constraints from apatite fission-track thermochronology. *J. Asian Earth Sc.*, **29,** 188-204.

Deng, Q.D., Zhang, P.Z., Xu, X.W., Yang, X.P., Peng, S.Z., and Feng, X.Y., 1996. Paleoseismology of the northern piedmont of Tianshan Mountains, northwestern China. *J. Geophys. Res.*, **101**, 5895-5920.

Dumitru, T.A., Zhou, D., Chang, E.Z., Graham, S.A., Hendrix, M.S., Sobel, E.R., and Caroll, A.R., 2001. Uplift, exhumation, and deformation in the Chinese Tian Shan. in: Paleozoic and

Mesozoic tectonic evolution of central Asia: From continental assembly to intracontinental deformation (Hendrix, M.S., and Davis,G.A., eds). *Geol. Soc. Am. Mem.*, **194**, 71–99.

Gao, J., Li, M.S., Xiao, X.C., Tang, Y.Q. and He, G.Q., 1998. Paleozoic tectonic evolution of the Tianshan Orogen, northwestern China. *Tectonophysics*, **287**, 213-231.

Graham, S.A., Hendrix, M.S., Wang, L.B. and Carroll, A.R., 1993. Collisional successor basins of western China Impact of tectonic inheritance on sand composition. *Geol. Soc. Am. Bull.*, **105**, 323-344.

Han B.F., He, G.Q. and Wang, S., 1999. Postcollisional mantle-derived magmatism, underplating and implications for basement of the Junggar Basin. *Sci. China. Ser. D*, **42**, 113-119.

Hendrix, M.S., Graham, S.A., Carroll, A.R., Sobel, E.R., Mcknight, C.L., Schulein, B.J., and Wang, Z.X., 1992. Sedimentary Record and Climatic Implications of Recurrent Deformation in the Tian-Shan - Evidence from Mesozoic Strata of the North Tarim, South Junggar, and Turpan Basins, Northwest China. *Geol. Soc. Am. Bull.*, **104**, 53-79.

Hendrix, M.S., Dumitru, T.A. and Graham, S.A., 1994. Late Oligocene Early Miocene Unroofing in the Chinese Tien-Shan - an Early Effect of the India-Asia Collision. *Geology*, **22**, 487-490.

Hendrix, M.S., 2000. Evolution of mesozoic sandstone compositions, southern Junggar, northern Tarim, and western Turpan basins, northwest China: A detrital record of the ancestral Tian Shan. *J. Sed. Res.*, **70**, 520-532.

Huang, B. and Li, J., 2007. Sporopollen assemblages from the Xishanyao and Toutunhe formations at the Honggou section of the manasi river, xinjiang and their stratigraphical significance. *Acta Micropaleontologica Sinica*, **24**, 170-193.

Jolivet, M., Ritz, J.F., Vassalo, R., Larroque, C., Braucher, R., Todbileg, M., Chauvet, A., Sue, C., Arnaud, N., de Vicente, R., Arzhanikova, A. and Arzhanikova, S., 2007. Mongolian summits: An uplifted, flat, old but still preserved erosion surface. *Geology*, **35**, 871-874.

Jolivet, M., Dominguez J., Charreau J., Chen, Y., Farley, K.A., Li, Y.A. and Wang, Q.C., 2010. Mesozoic and Cenozoic tectonic history of the Central Chinese Tian Shan: Reactivated tectonic structures and active deformation. *Tectonics*, **29**, TC6019, doi:10.1029/2010TC002712.

Laurent-Charvet S., Charvet, J., Shu, L.S., Ma, R.S. and Lu, H.F., 2002. Late Paleozoic collisional strike-slip deformations in Tianshan and Altay, eastern Xinjiang, NW China. *Terra Nova*, **14**, 249-256.

Li Z., Zhang L., Qian C., Wang Y. and Bai G., 1978. Regional geological survey report of Geological map 1:200000, Shichang sheet. China Ministry of Geology and Mineral Resource, Beijing.

Li, Z., Song, W.J., Peng, S.T., Wang, D.X. and Zhang, Z.P., 2004. Mesozoic-Cenozoic tectonic relationships between the Kuqa subbasin and Tian Shan, northwest China: constraints from depositional records. *Sed. Geol.*, **172**, 223-249.

Liu, Z., 1990. Sporo-pollen assemblage from Middle Jurassic Xishanyao Formation of Shawan, Xinjiang, China. *Acta Palaeontologica Sinica*, **29**, 63-82.

Lu Y.Z. and Deng S.W., 2005. Triassic-Jurassic Sporopollen Assemblages on the Southern Margin of the Junggar Basin, Xinjiang and the T-J Boundary. *Acta Geologica Sinica*, **79**, 15-28.

Martinod, J., and Davy, P., 1992. Periodic instabilities during compression of the lithosphere 1. Deformation modes from an analytical perturbation method. *J. Geophys. Res.*, **92**, 1999–2014.

Martinod, J. and Davy, P., 1994. Periodic instabilities during compression of the lithosphere 2. Analogue experiments. *J. Geophys. Res.*, **99**, 12057–12069.

Métivier, F. and Gaudemer, Y., 1997. Mass transfer between eastern Tien Shan and adjacent basins (central Asia): Constraints on regional tectonics and topography. *Geophys. J. Int.*, **128**, 1-17.

Sengör, A.M.C., Natal'in, B.A., Burtman, V.S., 1993. Evolution of the Altaid tectonic collage and Paleozoic crust growth in Eurasia. *Nature*, **364**, 299-307.

Sobel, E.R. and Dumitru, T.A., 1997. Thrusting and exhumation around the margins of the western Tarim basin during the India-Asia collision. *J. Geophys. Res.*, **102**, 5043-5063.

Tapponnier, P. and Molnar, P., 1977. Active Faulting and Tectonics in China. *J. Geophys. Res.*, **82**, 2905-2930.

Wang, B. Chen, Y., Zhan, S., Shu, L.S., Faure, M., Cluzel, D., Charvet, J. and Laurent-Charvet, S., 2007. Primary Carboniferous and Permian paleomagnetic results from the Yili Block (NW China) and their implications on the geodynamic evolution of Chinese Tian Shan Belt. *Earth Planet. Sci. Lett.*, **263**, 288-308.

Wang, Q. C., Li S. J. and Du z. L., 2009. Differential uplift of the Chinese Tian Shan since the Cretaceous: constraints from sedimentary petrography and apatite fission-track dating. *Int. J. Earth Sci.*, **98**, 1341-1363.

Wang, X.W., Wang, X.W., Liu, J.P., Liu, J.P. and Ma, Y.S., 2005. Analysis of the fold-thrust zone in the southern Junggar Basin , north western China. *Earth Science Frontiers*, **12**, 411-421.

Wang, Z., Wu, J., Lu, X., Liu, C., and Zhang, J., 1990, Polycyclic tectonic evolution and metallogeny of the Tian Shan mountains. Beijing, Science Press.

Windley, B.F., Allen, M.B., Zhang, C., Zhang, C., Zhao, Z.Y. and Wang, G.R., 1990. Paleozoic accretion and Cenozoic redeformation of the Chinese Tien Shan range, Central Asia. *Geology*, **18**, 128-131.

XBGMR-WUSU, 1973, Bureau of Geological and Mineral Resources of Xinjiang Uygur Autonomous Region, Geological map of Wusu Region, Scale 1:200.000, China Ministry of Geology and Mineral Resource, Beijing.

XBGMR-HOUXIA, 1977, Bureau of Geological and Mineral Resources of Xinjiang Uygur Autonomous Region, Geological map of Houxia Region, Scale 1:200.000, China Ministry of Geology and Mineral Resource, Beijing.

XBGMR-SHICHANG, 1978, Bureau of Geological and Mineral Resources of Xinjiang Uygur Autonomous Region, Geological map of Shichang Region, Scale 1:200.000, China Ministry of Geology and Mineral Resource, Beijing.

XBGMR, 1993, Regional geology of Xinjiang Uygur autonomy region.– Geological Memoirs, Ser. 1, No. 32, Map Scale 1: 1.500.000, Geological Publishing House, Beijing.

Yang, J., and Sun, S., 1982. The discovery of Early and Middle Jurassic megaspores from the Junggar Basin, Xinjiang, and their stratigraphic significance. *Acta Geologica Sinica*, **4**, 375–379.

Yang, J.L, Wang Q.F. and Lu H.N., 2005, Discovery of cretaceous and Paleocene charophyte floras from well Hu-2 in the southern edge of Junggar basin. Acta Micropalaeontologica Sinica, **22**, 251-268.

Figure captions

Fig. 1 Simplified geological map of the northern Tian Shan from Wusu to Urumqi areas. Mesozoic is most exposed in the southernmost parts of the Junggar basin along the adjacent Tian Shan range, particularly to the East (Urumqi area). 'He' indicates river in Chinese (modified after XBGMR, 1993).

Fig. 2 Synthetic and representative stratigraphic log made in the Manasi He area, northern Tian Shan piedmont, where Cenozoic have been widely eroded (modified after Hendrix et al., 1992).

Fig. 3 Landscape pictures of representative features of the Mesozoic sedimentary series (see locations on Fig.1) (a) Coarse-grained conglomerate of lowermost Jurassic forming prominent bars in the landscape (southern Qingshui He area); (b) Uppermost Jurassic coarse-grained breccias (Kalaza Fm. - J_{3k}) unconformably overlying the Upper Jurassic Qigu formation (J_{3q} ; Hutubi He area); (c) Close-up view of the Uppermost Jurassic Kalaza Fm. breccias (west to Hutubi He area). Note the angular shape of the clasts (locally exceeding 50 cm) and the clast-supported character of the coarser levels.

Fig. 4 Structural and sedimentological observations in the Houxia area. (a) Simplified geological map with some field structural measurements (modified after XBGMR, 1977), (b) detailed geological cross-section across the northern limb of the syncline structure (see location on Fig. 4a), (c) Close-up view of the Lower Jurassic breccias including Carboniferous basement angular clasts (see location on Fig. 4b), (d) picture of the steep bedding of Jurassic layers close to the southward thrust (see location on Fig. 4b).

Fig. 5 (a) Simplified geological map of the Hutubi He area (modified after XBGMR, 1978, 1993) with few structural measurements from field work. 'A' indicates location where Middle

Jurassic deposits directly and unconformity lie onto Carboniferous basement without Triassic or Lower Jurassic, (b) Geological cross-section along the Hutubi He constrained by field data, seismic profile (after Wang et al., 2005) and nearby drill wells W1 and W1'. Location of the section is indicated on Fig. 5a. Extension of the available seismic profile is indicated on the section.

Fig. 6 Examples of onlap structures of the Jurassic sediments over the Paleozoic basement units. (a) Picture and interpretation field sketch of the southern part of the Hutubi He (see location on Fig. 5a): note the overall southward onlap of the Jurassic sediments over the folded basement. To the north, a basement block is back thrusted over the sediments (see Fig. 5b), (b) Picture and interpretation field sketch of a small valley, west of the Hutubi He (see location on Fig. 5a): meso-scale basement relief covered by Jurassic sandstones as evidenced by onlaps over a steep inherited ~150 m high basement paleorelief (scarp). Basement rocks are deformed with a large inclined Paleozoic fold.

Fig. 7 Structural and sedimentological observations in the Wusu area. (a) Simplified geological map (modified after XBGMR, 1973) with few structural measurements. (b) Geological cross-section constrained by field data, seismic profile and drill well W2 (see Fig. 7a for location). (c) Picture and corresponding field sketch interpretation of the unconformable contact between Jurassic layers and the Carboniferous basement (see Fig. 7a for location).

Fig. 8 Sketch views of the paleogeographic evolution of the northern piedmont of Tian Shan during Early, Middle and Upper Jurassic/Cretaceous boundary. Main observations that constrain this study are localized on the drawings as: A for Fig. 3a; B for Fig. 4c (lower Jurassic sedimentary breccias); C for Fig. 6a (onlap covering of Paleozoic basement rocks by

Jurassic sandstones) and D for Figs. 3b and 3c (thick Kalaza Fm. breccias with angular discordance at the base).

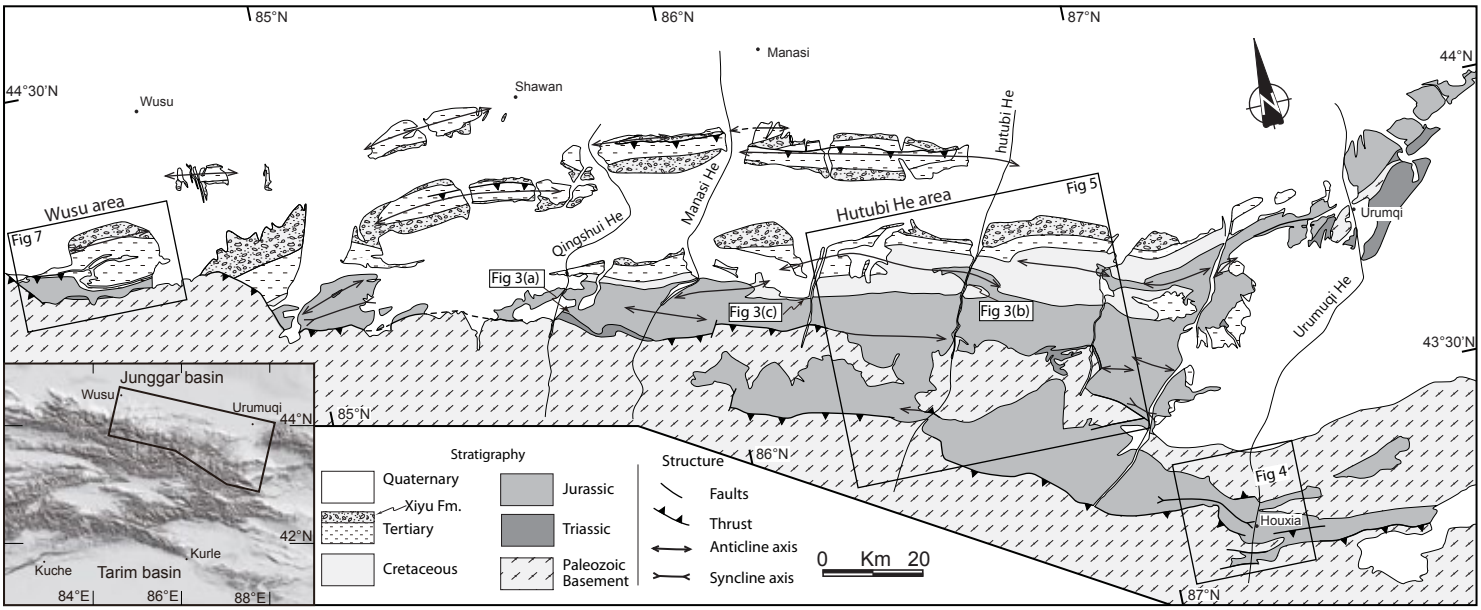
85°N
86°N
87°N
44°30'N
44°N
43°30'N
Wusu
Shawan
Manasi
Qingshui He
Manasi He
hutubi He
Urumqi
Urumuqi He
Wusu area
Fig 7
Hutubi He area
Fig 5
Fig 3(a)
Fig 3(c)
Fig 3(b)
Fig 4
Houxia
Junggar basin
Urumuqi
42°N
Kurle
Kuche
Tarim basin
84°E
86°E
88°E
Stratigraphy
Quaternary
Xiyu Fm.
Tertiary
Cretaceous
Jurassic
Triassic
Paleozoic Basement
Structure
Faults
Thrust
Anticline axis
Syncline axis
0 Km 20

Fig 1.

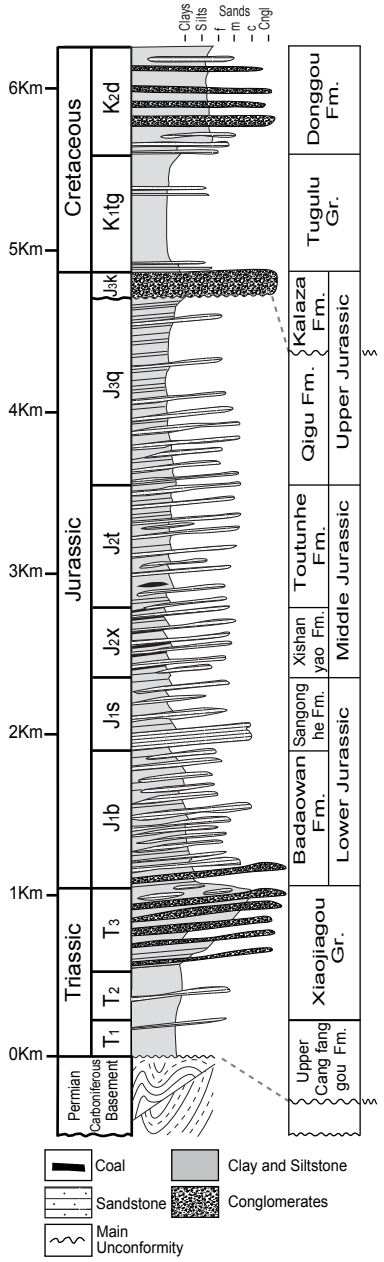
Clays
Silts
Sands
f
m
c
Congl
6Km
5Km
4Km
3Km
2Km
1Km
0Km
Cretaceous
Jurassic
Triassic
Permian
Carboniferous
Basement
K2d
K1tg
J3k
J3q
J2t
J2x
J1s
J1b
T3
T2
T1
Donggou Fm.
Tugulu Gr.
Kalaza Fm.
Qigu Fm.
Upper Jurassic
Toutunhe Fm.
Xishan yao Fm.
Middle Jurassic
Sangong he Fm.
Badaowan Fm.
Lower Jurassic
Xiaojiagou Gr.
Upper Cang fang gou Fm.
Coal
Clay and Siltstone
Sandstone
Conglomerates
Main Unconformity

Fig 2.

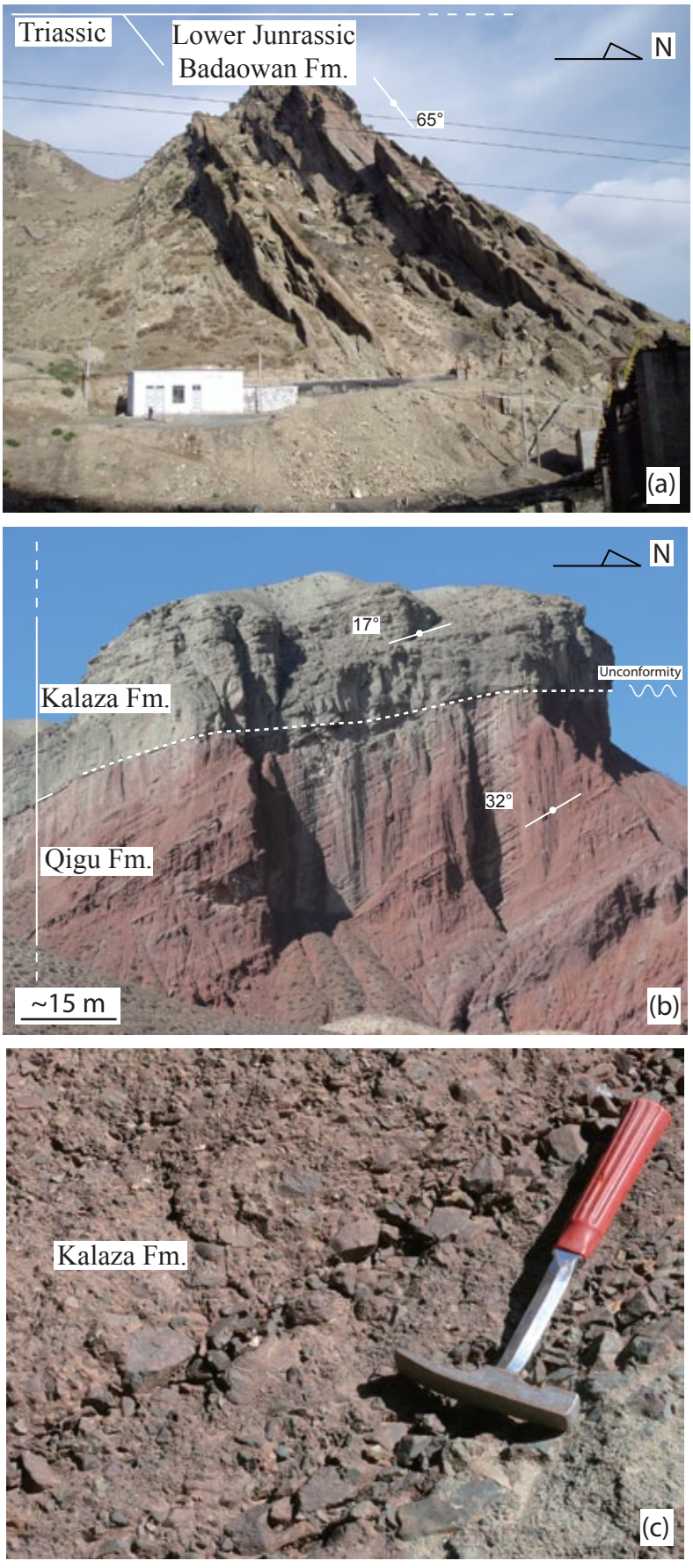
Triassic
Lower Junrassic
Badaowan Fm.
N
65°
(a)
N
17°
Unconformity
Kalaza Fm.
32°
Qigu Fm.
~15 m
(b)
Kalaza Fm.
(c)

Fig 3.

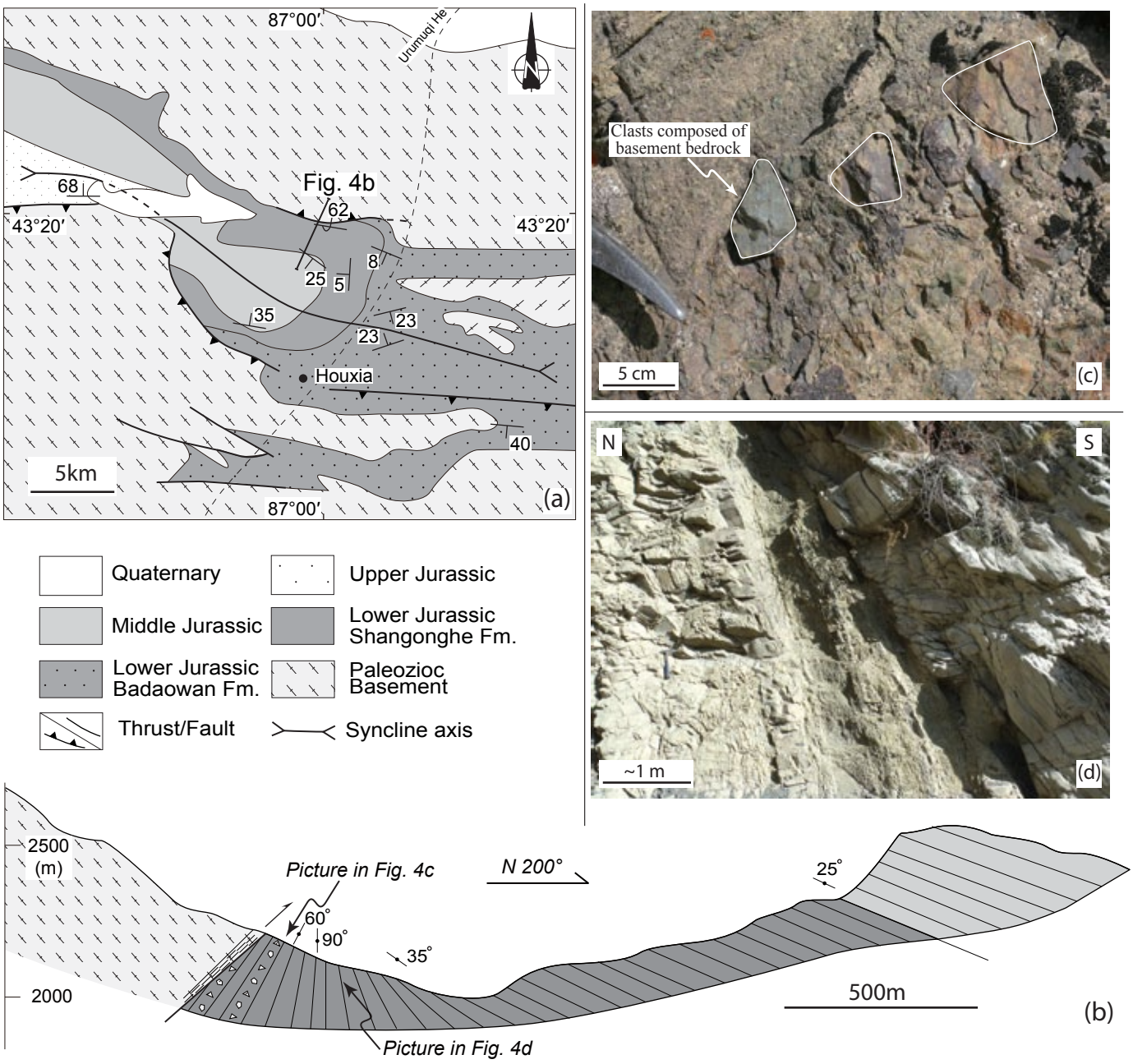
87°00′
Urumuqi He
N
Fig. 4b
68
62
43°20′
43°20′
8
25
5
35
23
23
Houxia
40
5km
87°00′
(a)
Clasts composed of basement bedrock
5 cm
(c)
N
S
~1 m
(d)
Quaternary
Upper Jurassic
Middle Jurassic
Lower Jurassic Shangonghe Fm.
Lower Jurassic Badaowan Fm.
Paleozioc Basement
Thrust/Fault
Syncline axis
2500 (m)
Picture in Fig. 4c
N 200°
25°
60°
90°
35°
2000
500m
(b)
Picture in Fig. 4d

Fig 4.

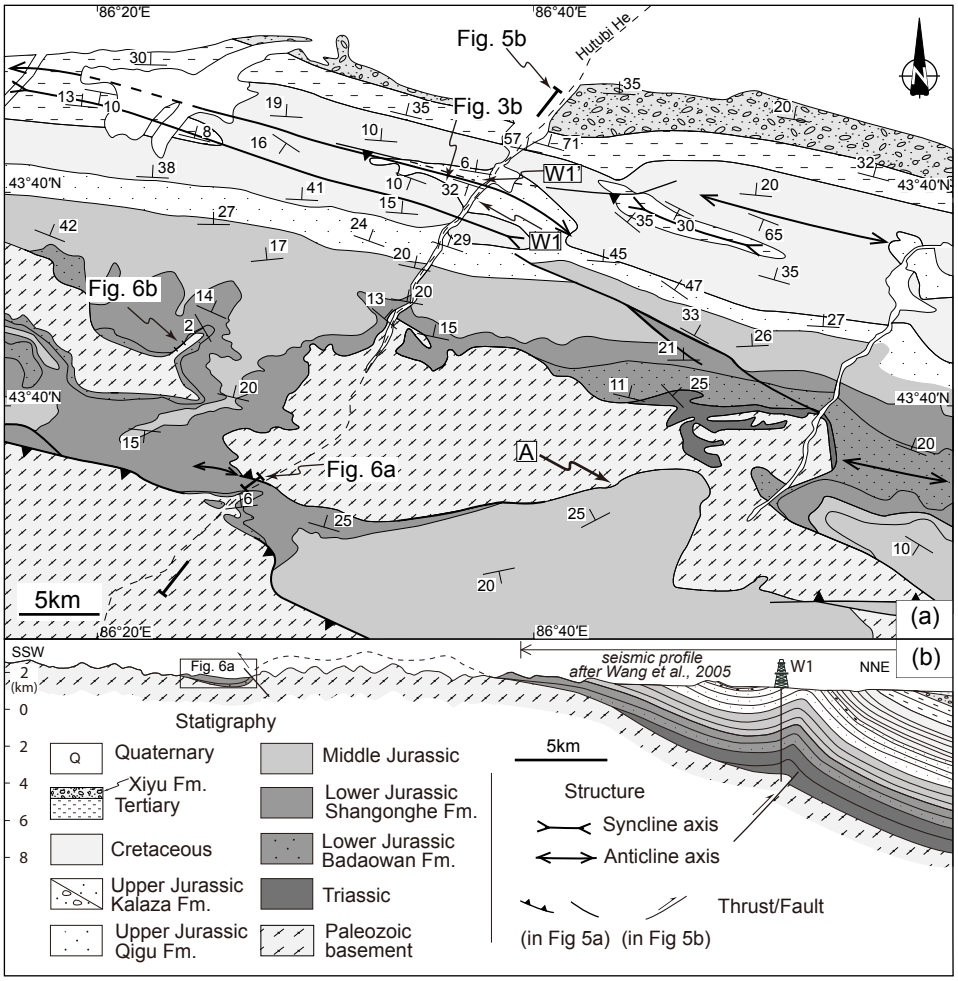
86°20'E
86°40'E
Hututbi He
Fig. 5b
Fig. 3b
Fig. 6b
Fig. 6a
W1
A
43°40'N
5km
(a)
(b)
SSW
NNE
seismic profile
after Wang et al., 2005
Statigraphy
Quaternary
Xiyu Fm.
Tertiary
Cretaceous
Upper Jurassic
Kalaza Fm.
Upper Jurassic
Qigu Fm.
Middle Jurassic
Lower Jurassic
Shangonghe Fm.
Lower Jurassic
Badaowan Fm.
Triassic
Paleozoic
basement
Structure
Syncline axis
Anticline axis
Thrust/Fault
(in Fig 5a) (in Fig 5b)

Fig 5.

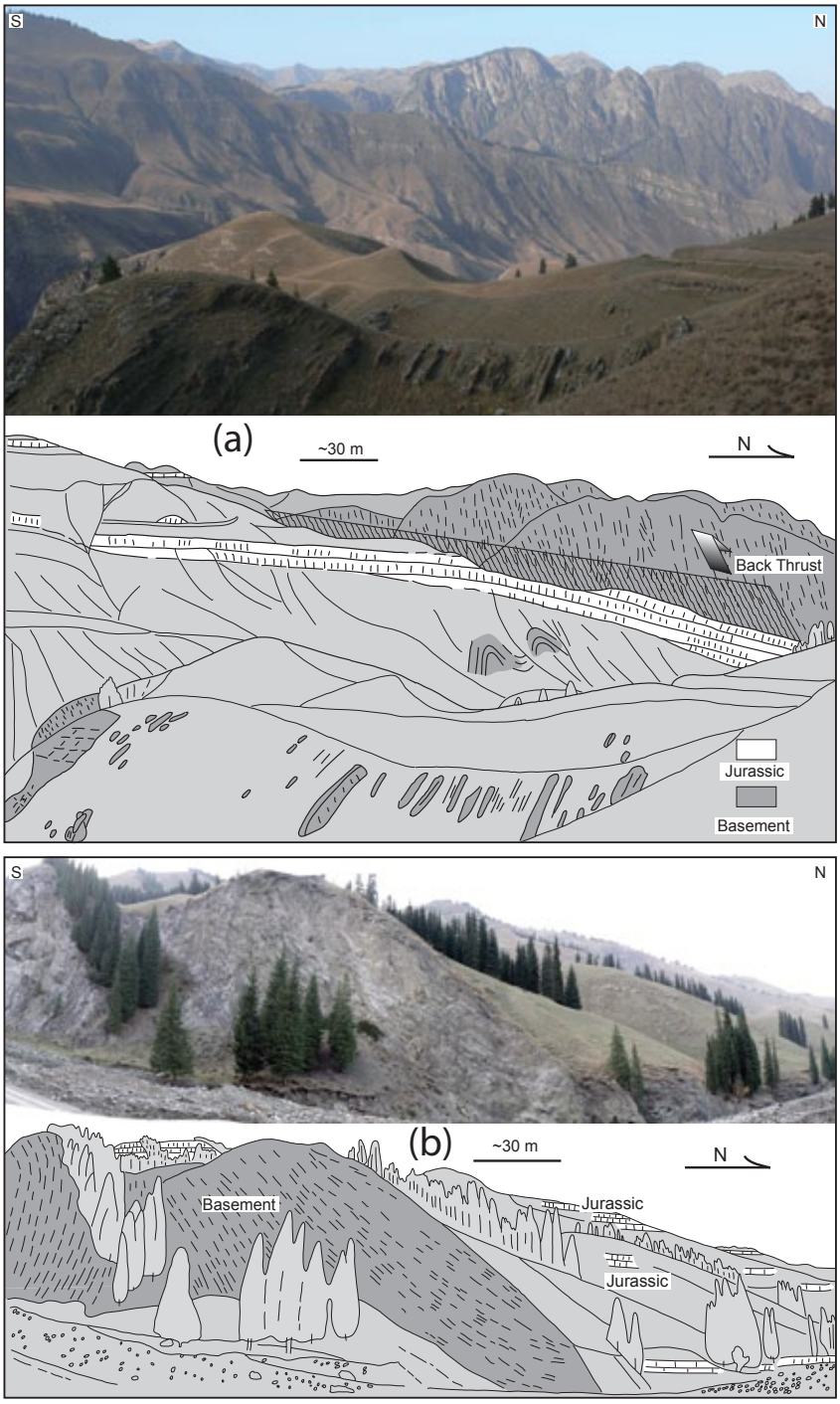
S
N
(a)
~30 m
N
Back Thrust
Jurassic
Basement
S
N
(b)
~30 m
N
Basement
Jurassic
Jurassic

Fig 6.

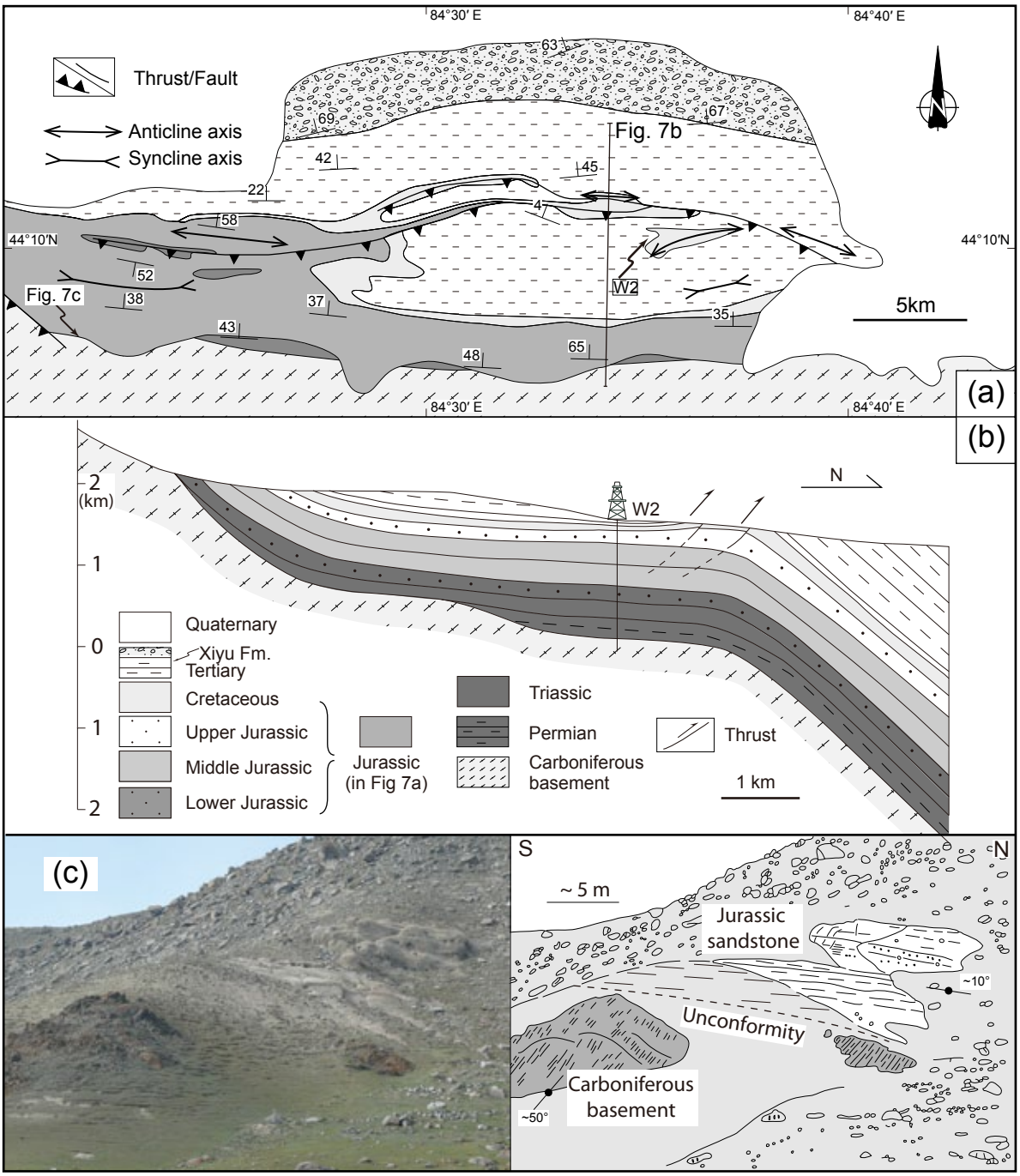
84°30′ E
84°40′ E
Thrust/Fault
Anticline axis
Syncline axis
Fig. 7b
Fig. 7c
44°10′N
W2
5km
(a)
(b)
2
(km)
1
0
1
2
N
Quaternary
Xiyu Fm.
Tertiary
Cretaceous
Upper Jurassic
Middle Jurassic
Lower Jurassic
Jurassic
(in Fig 7a)
Triassic
Permian
Carboniferous
basement
Thrust
1 km
(c)
S
N
~ 5 m
Jurassic
sandstone
~10°
Unconformity
Carboniferous
basement
~50°

Fig 7.

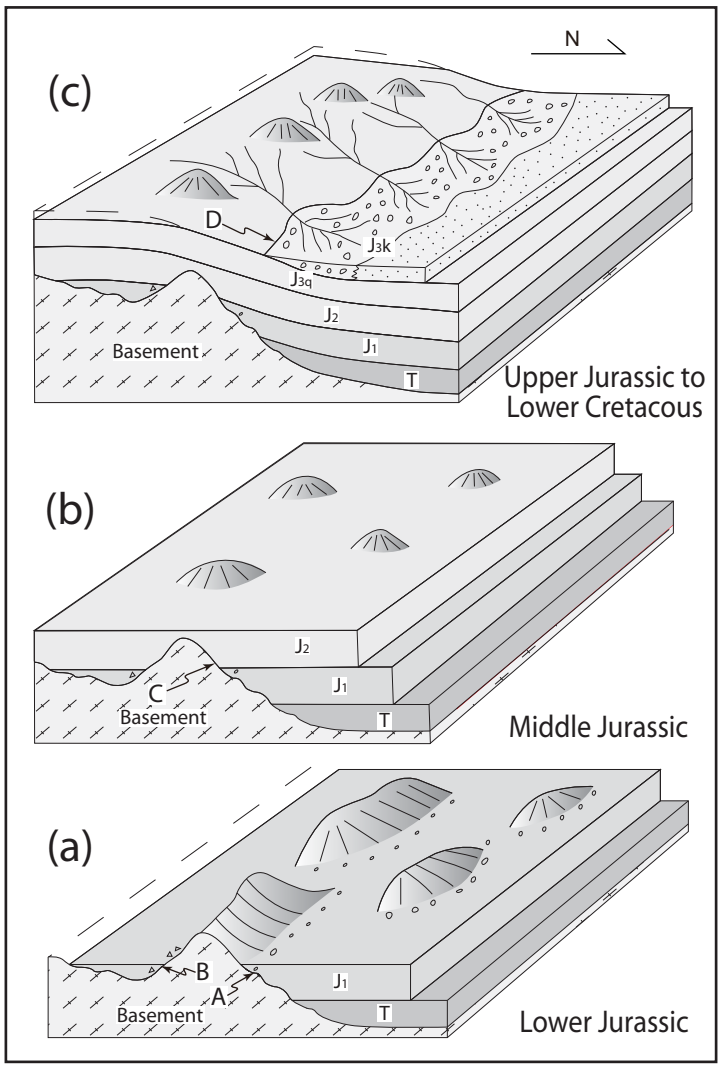
N
(c)
D
J3k
J3q
J2
J1
T
Basement
Upper Jurassic to
Lower Cretacous
(b)
J2
J1
T
C
Basement
Middle Jurassic
(a)
B
A
J1
T
Basement
Lower Jurassic

Fig 8.

The Mesozoic paleorelief of the northern Tian Shan (China)

Ke CHEN[1,2], Charles GUMIAUX[1], Romain AUGIER[1], Yan CHEN[1], Qingchen WANG[2] , Wei LIN[2] , Shengli WANG[3] ,

1. Institut des Sciences de la Terre d'Orléans (ISTO), Université d'Orléans, CNRS: UMR6113, Université François Rabelais - Tours, - INSU, Campus Géosciences, 1A rue de la Férollerie, 45071 Orléans cedex 2, France

2. State Key Laboratory of Lithospheric Evolution, Institute of Geology and Geophysics, Chinese Academy of Sciences, P.O. 9825, Beijing 100029, China

3. Department of Earth Sciences, Nanjing University, 210093, Nanjing, China

Abstract

The Tian Shan range offers a natural laboratory to study orogenic processes. Most of the previous studies focused on either the Paleozoic evolution of the range or its Cenozoic intracontinental evolution linked with the India-Asia collision. In this study, detailed field investigations on the relationship between sedimentary cover and basement constrain the Mesozoic evolution of the northern Tian Shan. Sedimentological observations argue for limited transport distance for Lower and Uppermost Jurassic deposits. Geological sections presented in this paper show that, in preserved locations, Triassic to Jurassic sedimentary series present a continuous onlap type sedimentary unconformity on the top of the basement. At different scales, observations clearly evidence the existence of a major paleorelief during Mesozoic. According to the present study, the current Tian Shan range topography and the associated movements along its northern front structures cannot be considered as the consequence of Cenozoic reactivation alone.

Keywords

Tian Shan, paleorelief, Mesozoic, regional onlap, reactivation, India-Asia collision.

Introduction

The modern Tian Shan is one of the major mountain ranges in Central Asia. The current structure of Tian Shan mainly results from a combination of two main tectonic events: i) subductions, arc-accretions and continental collision during Paleozoic (e.g. Carroll et al., 1990; Wang et al., 1990; Windley et al., 1990; Sengör et al. 1993; Carroll et al., 1995; Gao et al., 1998; Laurent-Charvet et al., 2002; Charvet et al., 2007; Wang et al., 2007) and ii) intracontinental reactivation linked to the India-Asia collision, during Cenozoic (e.g. Tapponnier and Molnar, 1977; Avouac et al., 1993). At first order, the modern Tian Shan corresponds to a raised ~east-west trending Paleozoic 'basement' range, flanked by two closed intracontinental basins whose infill is a particularly accurate record for both tectonic and climate evolutions (Fig. 1). The present-day high topography of Tian Shan, with a mean altitude of ~2500 m and summits of more than 7000 m, is traditionally related to the latest intracontinental deformation of the range (e.g. Tapponnier and Molnar, 1977; Avouac et al., 1993; Burchfiel et al., 1999). Age constraints for the onset of this intracontinental reactivation range from 10 to 24 Ma (e.g. Avouac et al., 1993; Hendrix et al., 1994; Abdrakhmatov et al., 1996; Métivier and Gaudemer, 1997; Sobel et al., 1997; Dumitru et al., 2001; Charreau et al., 2009). In spite of relative age discrepancies (mostly related to the method applied), all ages estimated for the deformation and the associated relief erosion suggest that the mountain range reactivation and relief creation began during Early Miocene at oldest.

However, recent Fission-track analyses suggest that uplifting may have existed well before the onset of the Tertiary reactivation through Tian Shan, with exhumation ages such as 160-120 Ma in central Tian Shan, 200-250 Ma detritus cooling age in the Manas River valley (Dumitru et al., 2001; Jolivet et al., 2010) or 140-120 Ma from Bayanbulak intracontinental basin, in the southern Tian Shan (Wang et al., 2009). Moreover, Triassic to Cretaceous sediments are composed of thick continental series characterized by massive coarse-grained

formations within both basins, suggesting rather high erosion rate at that time (Hendrix, 2000; Carroll et al., 2010).

This study considers the Mesozoic tectonic and morphologic evolution of Tian Shan through field structural and sedimentological analyses of Mesozoic deposits. It focuses on the northern piedmont of the range, along a ~280 km west-east trending segment (Fig. 1). Thanks to deep incisions of seasonal rivers, contacts between Paleozoic basement and Mesozoic-Cenozoic sedimentary cover are particularly well exposed along several north-south trending sections in this region (Fig. 1). Such new constraints on Mesozoic evolution of the Tian Shan area would lead to reconsider the contribution of Cenozoic tectonics in the modern mountain range building as well as to better quantify the net shortening amount during that period.

Stratigraphy of the Mesozoic sediments within the study area

Sedimentary series can be extensively observed and have already been studied within the Junggar basin, as summarized below (Figs. 1 and 2; Hendrix et al., 1992 and references therein; XBGMR, 1993). Basement units of the north Tian Shan mainly consist of Paleozoic volcanic and sedimentary rocks. From bottom to top, the entire Mesozoic series is composed of ~5 km thick continental clastic deposits highlighting high sedimentation/preservation rates (Fig. 2). Thanks to numerous studies aimed at oil and gas exploration and to 1:200.000 mapping projects hold in this area, ages of the Mesozoic sequences were mainly constrained by floral and sporopollen assemblage analyses (Li et al., 1978; Yang et al., 1982; Liu, 1990; XBGMR, 1993; Lu and Deng, 2005; Yang et al., 2005; Huang and Li, 2007). In the study area, the Triassic series are mostly missing along the piedmont though locally exposed (Fig. 1). Where it crops out, Triassic displays alluvial sandstones and conglomerates intercalated within and silty mudstones (red-beds). At the scale of the northern Tian Shan piedmont, Lowermost Jurassic layers indicate a change in the sedimentation as they consist in thick and

coarse conglomeratic deposits, as exposed in the south of Qingshui He (Fig. 3a). Thickness of Lower Jurassic reaches 1000 m over the area extending from Manasi to Urumqi, and decreases westwardly and eastwardly. Sediments become progressively finer upward, grading into ~3 km thick series of Lower/Middle Jurassic gray sandstones, silty shales (Fig. 2). Middle Jurassic sandstones and mudstones locally contain coal-rich layers consistent with a lacustrine depositional facies (Hendrix et al., 1992). Upper Jurassic comprises typical fine-grained red beds where conglomerates remain scarce. The transition from Jurassic to Cretaceous series is marked by up to 800 m thick sedimentary breccias (Kalaza formation – J3k; Fig. 3b) made of coarse-grained angular clasts (Fig. 3c). It rapidly dies laterally and grades to sandstones within the Junggar basin itself (XBGMR, 1978; 1993). The marked unconformity between the Kalaza formation and the underlying finer-grained Upper Jurassic red beds (Fig. 3b) suggests a short transport distance of material before deposition and nearby relief uplifting.

In this study, Mesozoic sediments have also been extensively observed within internal parts of the range, and more particularly in the eastern part of the studied area (Fig. 1). Triassic to Jurassic sediments are encountered on top of the Paleozoic basement units, at rather high altitudes (2000 to 3000 m) in comparison with the mean altitude of the foreland fold-and-thrust belts (1000 to 1500 m high). In the Houxia valley for instance – 65 km SSW of Urumqi – a Lower to Upper Jurassic continuous sedimentary series is preserved in a syncline structure (Fig. 4a). According to the geological map (Fig. 4a; XBGMR, 1977), Lower Jurassic formations – i.e. Shangonghe Fm. to the northwest and Lowermost Jurassic Badaowan Fm. to the east – directly overlie on top of Carboniferous basement units, without intercalated Triassic sediments. Besides, south and north verging thrusts developed along parts of the northern and southern limbs of the fold, respectively (Fig. 4a). A section made across the north limb of the syncline displays continuous Lower to Middle Jurassic series with

no fault contact observed (Fig. 4b). From south to north, bedding planes progressively straighten up from ~30° south dipping to vertical, and even overturned just below the south verging thrust (Figs. 4a ,4b and 4d). From a sedimentological point of view, the upper and main part of Jurassic series is made of fine-grained sandstones and mudstones while the lowermost deposits of the series is characterized by intercalations of coarse-grained sedimentary breccias mostly made of highly angular clasts of Carboniferous tuffaceous sandstones (Fig. 4c). Local abundance of these breccias and the common lithological nature of the clasts with the adjacent basement unit strongly suggest a very short transport distance.

Structural analysis of the Mesozoic basal contact

Deformation of the northern Tian Shan has already been studied through the structural analysis of sedimentary series, within the Cenozoic foreland basin (e.g. Avouac et al., 1993; Deng et al., 1996; Burchfiel et al., 1999). This part focuses on the basal contact of the Mesozoic sediments, in the northern “front” area of Tian Shan.

As shown on the map (Fig. 1), some parts of the piedmont display northward thrusts that mark out the boundary in between the Paleozoic uplifted basement units and relatively subsiding proximal foreland basin. Yet, as described above, Mesozoic series are not solely restricted to the piedmont fold-and-thrust belts but are also well preserved on top of the basement units, within the range (Fig. 1). Then, some other segments of the piedmont display perfectly continuous Mesozoic sedimentary series from basin until internal and higher parts of the range, without being strained by any faulting or folding in the range front area (Fig. 1). Structural analysis of such unstrained basal contact of Mesozoic series is presented for two of the sections constructed from field work combined with available seismic profiles and drill-holes data: the Hutubi He and the Wusu sections (Fig. 1).

120 At first order, to the north of the Hutubi He area, Triassic to Neogene sedimentary
121 series form a rather simple monocline structure, dipping 15-20° to the north (Fig. 5a). The
122 southernmost fold-and-thrust belt is composed of one gentle upright anticline and associated
123 syncline with only very limited thrusts developed along the hinge of the fold (Fig. 5a). This
124 belt can be regarded as a fault-propagation fold structure according to the available seismic
125 profile (Wang et al., 2005; Fig. 5b). Further south, entering within the interior parts of the
126 range, sub-horizontal Lower Jurassic strata lie on top of the Carboniferous units (Fig. 5b).
127 While basement is strongly deformed, as evidenced by sub-vertical cleavage, its sedimentary
128 cover is only gently folded as illustrated on the geological map, few kilometers west of the
129 river (Fig. 5a; XBGMR, 1978, 1993). No décollement structure has been observed between
130 the basement top and the sedimentary cover. Besides, a southward backthrust of basement
131 rocks above sediments can be observed to the south of the section, but the net slip must be
132 limited as it rapidly dies out, the fault laterally evolving to a fold toward the west (Fig. 5a).
133 Unconformity of the basal contact of Mesozoic sediments on top of basement units is
134 observed in the southernmost part of the section (Figs. 5a and 6a). As a whole, the successive
135 sub-horizontal and monocline segments define a hinge fold at regional scale (Fig. 5b).
136 Nevertheless, while ~900 m thick of Triassic sediments have been drilled along the W1 well
137 in the basin (Fig. 5b), no Triassic series have been observed further south in the range, in the
138 section area (Fig. 5a). Indeed, Lowermost to Middle Jurassic levels have been observed and
139 mapped directly on top of the basement units (Fig. 5a; XBGMR, 1978, 1993). Similarly to the
140 Houxia area, basal contact of the Mesozoic series suggests its onlap deposit, from basin to
141 range, at least during Triassic and Lower-Middle Jurassic.

142 More local-scale evidences for onlap sedimentation can also be observed in the Hutubi
143 He area. First, to the south end of the section, Lower Jurassic strata display a kilometer scale
144 onlap type structure on top of basement units, i.e. with younger sediments progressively

covering basement, from north to south (Figs. 5a and 6a). Second, ~10 km west of the Hutubi River, subhorizontal layers of the Lower Jurassic formation, which can be continuously followed in few kilometers in this small valley, structurally onlap on the deformed Paleozoic basement units (Fig. 6b). There, stratification planes are markedly oblique with the top of the Paleozoic units and no deformation has been observed along this contact. In the landscape, younger Jurassic sediments progressively extend to the south, on top of the Carboniferous units. Sediments progressively overlie and cover a ~150 m high step of the basement top which implies that a significant relief existed during Jurassic sediments deposition.

To the north of the Wusu section, first-order structure of the Mesozoic-Cenozoic series displays a 40-45° north dipping monocline (Figs. 7a and 7b). To the south, bedding is sub-horizontal and structure of the sedimentary series is marked by a large hinge fold. As drawn on the geological map, thrust faults are observed at the surface, but seismic data show that they do not extend downward into the Mesozoic series (Fig. 7b; *suppl. material*), which is compatible with the limited throw produced by these faults as deduced from map data analysis (Fig. 7a). While ~400 m of Triassic sediments have been found in a drilled well in the basin, close to this section (see W2 on Fig. 7a), Triassic series becomes much thinner to the south and Jurassic sandstones, sometimes, directly lie on top of the Carboniferous rocks with an erosional undeformed contact (Fig. 7c; XBGMR, 1973).

Discussion and conclusions

In parallel to rather classical view of frontal thrust systems, this study highlights that the northern piedmont of Tian Shan also displays segments where Mesozoic series are preserved unconformably onto the basement with onlap-type relationships. Such features are pointed out along two distant cross-sections and have also been clearly shown at outcrop-scale. Sedimentary breccias, showing very limited transport distances, have been found within

Lower Jurassic sediments of the internal parts of the range. Whatever the scale, all these observations clearly show the existence of proximal relief when Triassic/Jurassic sediments were deposited. Our field observations are consistent with previously published sedimentological data – paleocurrent measurements, heavy mineral composition, sedimentological source analyses – in the Junggar and Tarim basins which suggest that Tian Shan could already have existed as a "positive" geomorphologic feature during Mesozoic times (Hendrix et al., 1992, Graham et al., 1993; Hendrix, 2000; Li et al., 2004).

In the field, the local-scale observation of onlap sedimentary architecture reveals that the paleo-altitude difference can reach 100-150 m in a hectometer horizontal distance, which highlights local steep slopes (cf. Fig. 6b). Together with the sedimentological observations in the Houxia valley, this suggests that small-scale ridges with intercalated intra-mountainous basins have probably existed during Mesozoic (Fig. 8a).

Drill wells W1 and W1' (Figs. 4a and 4b) display ~1200 m of Lower Jurassic sediments (e.g. Badaowan and Shangonghe Fm., Fig. 2). A comparable thickness for Lower Jurassic has also been observed in the Manas area, 50 km west of the Hutubi section (Fig. 2; Hendrix et al., 1992). Following the geological maps (XBGMR; 1978, 1993), Middle Jurassic series directly lie unconformably onto the Carboniferous basement, without Triassic and Lower Jurassic sediments in the southern part of the Hutubi River (see location A in Fig. 4a). The thickness difference of Jurassic sediments reaches ~1200 m between the location A and the drill well location, for a horizontal distance of about 50 km (Fig. 4a). Such thickness difference may result from subsidence mechanisms. However, whatever the scale considered in this study, Triassic and mostly Jurassic series, up to the late Jurassic Kalaza formation deposit, display parallel bedding with no growth strata observed (Figs. 5b, 6 and 7b). Such feature shows that, at the scale of the studied area, significant vertical differential movements may have hardly occurred during Triassic to Upper Jurassic sedimentation. In addition, as

described above, Jurassic strata often overlie directly on Carboniferous by onlap, without fault or syn-sedimentary deformations. Seismic profiles across the southern margin of the Junggar basin do not display major fault that could have controlled sedimentation for the Early Jurassic period (Allen et al., 1991; Wang et al., 2005). No evidence for structural control on local subsidence could thus be argued here. At larger scale, flexure – either thermal or tectonic – could also have controlled the subsidence for Mesozoic series accumulation.

If considering thermal control, the latest regional tectono-magmatic event occurring before Mesozoic in the Central Tian Shan area ended during early Permian (see compilation by Han et al., 1999), which is about 100 Ma earlier than Jurassic sedimentation. Therefore, according to Hendrix et al. (1992), it seems that thermal driving mechanism may only play a weak role for the Early and Middle Jurassic sedimentation. If considering tectonic control, compressional flexure may also be hard to explain as, for comparable vertical differential movements, buckling of a stable continental lithosphere would result in much larger wavelength (200-300 km) than observed in this study (~50 km) as shown by mechanical modelling (Martinod and Davy, 1992, 1994; Burov et al., 1993; Cloetingh et al., 1999).

At the scale of the present study, Jurassic sedimentation seems hardly controlled by either tectonic or thermal subsidence across northern Tian Shan. Accordingly, the 1200-1300 m thickness difference may be mainly produced by infilling of a long-lasting remnant relief of, at least, 1200-1300 m high at that period (i.e. from Triassic/Lowermost Jurassic; Fig. 8a). During Middle Jurassic, finer-grained sediments were conformably deposited on top of the Lower Jurassic strata within the basin, and were deposited onlap on the Paleozoic basement toward the range (Figs. 5a and 8b). Middle Jurassic sediments of the Xishanyao and Toutunhe formations extend to a larger area with respect to the Lower Jurassic and, as a whole, the paleorelief lateral extension was certainly less important during Middle Jurassic than during Triassic/Early Jurassic (Fig. 8b). During latest Jurassic to Early Cretaceous, thick

219 breccias were deposited onto the Middle Jurassic sediments through an angular unconformity
220 (*cf.* Kalaza Fm.). These breccias are restricted to the front of the modern Tian Shan and
221 change rapidly to finer-grained deposits in lateral equivalents. This configuration is
222 reminiscent of the general architecture of current fans deposited along the modern Tian Shan
223 range that originate from the present day high relief to the south, but show limited northward
224 transport of sediments (Fig. 8c). In turn, location of the main morphological northern front of
225 the paleo- Tian Shan, during Latest Jurassic to Early Cretaceous, would approximately
226 coincide with the one of the current range front (Fig. 5). The uplift documented by these
227 coarse-grained sedimentary breccias is also recorded by AFT chronology studies; Fission-
228 track modeling indicates a ca. 160 and 120 Ma cooling age along a Dushanzi-Kuqa corridor,
229 in the mountain interior (Dumitru et al., 2001; Jolivet et al., 2010). Apatite sampled from
230 Bayanbulak area yields the earliest cooling ages of Early Cretaceous (Dumitru et al., 2001;
231 Wang et al. 2009).

232 Because no major tectonic event occurred in the Northern Tian Shan during Mesozoic
233 times (e.g. De Grave et al., 2007), the Paleozoic subduction-collision orogeny (Gao et al.,
234 1998; Laurent-Charvet et al., 2002; Charvet et al., 2007) appears as the most probable origin
235 of the Mesozoic paleorelief above described. In such case, the Tian Shan would persist as
236 remnant relieves for several tens of Ma after the end of the orogenic events which are
237 progressively and unconformably overlain by Triassic and then Jurassic sedimentation (e.g.
238 onlap structures, mesoscale paleorelief infilling). This scenario implies extremely low erosion
239 rates to allow the preservation of a significant relief; such feature has already been reported
240 for other regions of Central Asia from thermochronological (AFT) and field data analyses
241 (Jolivet et al., 2007). In parallel, Central Asia Mesozoic tectonic history is marked by the
242 polyphased Cimmerian orogeny in Tibet area (e.g. Hendrix et al., 1992; Sobel and Dumitru,
243 1997; De Grave et al., 2007). Low amplitude, far-field effects can thus be recognized in the

Mesozoic northern Tian Shan: one early collision stage – Qiantang/Kunlun blocks during Late Triassic/Middle Jurassic – would correspond to the drastic coarsening of the Lower Jurassic sedimentation. In turn, a later collision stage – Lhasa/Qiantang blocks during Late Jurassic/Early Cretaceous – well corresponds to the deposits of the thick and coarse breccias of the Kalaza Fm. at that time. In this case, a tectonic origin of the relief rejuvenation is attested by a major angular unconformity observed regionally.

As unambiguously demonstrated, the physiography of the modern Tian Shan dominantly results from the recent tectonic evolution of the area (e.g. Tapponnier and Molnar, 1977; Avouac et al., 1993; Métivier and Gaudemer, 1997; Charreau et al., 2009). However, this study put forward that the current Tian Shan topography can probably not be considered as the consequence of the Cenozoic intracontinental reactivation alone, but as a combination of the Cenozoic deformations superimposed on a reminiscent Mesozoic paleo-range. These new results question on the amplitude of the movements that could be estimated along the northern front structures during Cenozoic intracontinental reactivation.

Acknowledgements

Field and laboratory work in the present study are financially supported by Chinese National 973 Program (2009CB825008) and Chinese National S&T Major Project 2011ZX05008. Prof. A.R. Caroll, Dr. J. Charreau, and an anonymous reviewer are warmly thanked for their constructive reviews. We are also grateful for the help by Prof. Carlo Doglioni (*Editor*) and Prof. Gerhard Wörner (*Associate Editor*). Discussions on seismic profiles' interpretation with Dr. Y. Branquet have also been greatly appreciated. The first author benefices a Ph.D scholarship from French Embassy in Beijing and IGGCAS.

References

Abdrakhmatov, K.Y., Aldazhanov, S.A., Hager, B.H., Hamburger, M.W., Herring, T.A., Kalabaev, K.B., Makarov, V.I., Molnar, P., Panasyuk, S.V., Prilepin, M.T., Reilinger, R.E., Sadybakasov, I.S., Souter, B.J., Trapeznikov, Y.A., Tsurkov, V.Y. and Zubovich, A.V., 1996. Relatively recent construction of the Tien Shan inferred from GPS measurements of present-day crustal deformation rates. *Nature*, **384**, 450-453.

Allen, M.B., Windley, B.F., Zhang, C., Zhao, Z.Y. and Wang, G.R., 1991. Basin Evolution within and Adjacent to the Tien-Shan Range, NW China. *J. Geol. Soc. London*, **148**, 369-378.

Avouac, J.P., Tapponnier, P., Bai, M., You, H. and Wang, G., 1993. Active Thrusting and Folding Along the Northern Tien-Shan and Late Cenozoic Rotation of the Tarim Relative to Dzungaria and Kazakhstan. *J. Geophys. Res.*, **98**, 6755-6804.

Burchfiel, B.C., Brown, E.T., Deng, Q.D., Feng, X.Y., Li, J., Molnar, P., Shi, J.B., Wu, Z.M. and You, H.C., 1999. Crustal shortening on the margins of the Tien Shan, Xinjiang, China. *Int. Geol. Rev.*, **41**, 665-700.

Burov, E.B., Lobkovsky, L.I., Cloetingh, S. and Nikishin, A.M., 1993. Continental lithosphere folding in Central Asia (Part II): constraints from gravity and topography. *Tectonophysics*, **226**, 73–87.

Carroll, A.R., Liang, Y., Graham, S.A., Xiao, X., Hendrix, M.S., Chu, J., and McKnight, C.L., 1990. Junggar basin, northwest China: Trapped late Paleozoic ocean. *Tectonophysics*, **181**, 1-14.

Carroll, A. R., Graham, S.A., Hendrix, M.S., Ying, D., and Zhou, D., 1995. Late Paleozoic tectonic amalgamation of northwestern China: sedimentary record of the northern Tarim, northwestern Turpan, and southern Junggar basins. *Geol. Soc. Am. Bull.*, **107**, 571-594.

Carroll, A.R., Graham, S.A. and Smith, M.E., 2010. Walled sedimentary basins of China. *Basin Res.*, **22**, 17-32.

Charreau, J., Chen, Y., Gilder, S., Barrier, L., Dominguez, S., Augier, R., Sen, S., Avouac, J.P., Gallaud, A., Graveleau, F. and Wang, Q.C., 2009. Neogene uplift of the Tian Shan Mountains observed in the magnetic record of the Jingou River section (northwest China). *Tectonics*, **28**, TC2008, doi:10.1029/2007TC002137.

Charvet, J., Shu, L.S. and Laurent-Charvet, S., 2007. Paleozoic structural and geodynamic evolution of eastern Tianshan (NW China): welding of the Tarim and Junggar plates. *Episodes*, **30**, 162-186.

Cloetingh, S., Burov, E. and Poliakov, A., 1999. Lithosphere folding: primary response to compression? (from central Asia to Paris basin). *Tectonics*, **18**, 1064–1083.

De Grave, J., Buslov, M.M. and Van den Haute, P., 2007. Distant effects of India–Eurasia convergence and Mesozoic intracontinental deformation in Central Asia: Constraints from apatite fission-track thermochronology. *J. Asian Earth Sc.,* **29,** 188-204.

Deng, Q.D., Zhang, P.Z., Xu, X.W., Yang, X.P., Peng, S.Z., and Feng, X.Y., 1996. Paleoseismology of the northern piedmont of Tianshan Mountains, northwestern China. *J. Geophys. Res.*, **101**, 5895-5920.

Dumitru, T.A., Zhou, D., Chang, E.Z., Graham, S.A., Hendrix, M.S., Sobel, E.R., and Caroll, A.R., 2001. Uplift, exhumation, and deformation in the Chinese Tian Shan. in: Paleozoic and

Mesozoic tectonic evolution of central Asia: From continental assembly to intracontinental deformation (Hendrix, M.S., and Davis,G.A., eds). *Geol. Soc. Am. Mem.*, **194**, 71–99.

Gao, J., Li, M.S., Xiao, X.C., Tang, Y.Q. and He, G.Q., 1998. Paleozoic tectonic evolution of the Tianshan Orogen, northwestern China. *Tectonophysics*, **287**, 213-231.

Graham, S.A., Hendrix, M.S., Wang, L.B. and Carroll, A.R., 1993. Collisional successor basins of western China Impact of tectonic inheritance on sand composition. *Geol. Soc. Am. Bull.*, **105**, 323-344.

Han B.F., He, G.Q. and Wang, S., 1999. Postcollisional mantle-derived magmatism, underplating and implications for basement of the Junggar Basin. *Sci. China. Ser. D*, **42**, 113-119.

Hendrix, M.S., Graham, S.A., Carroll, A.R., Sobel, E.R., Mcknight, C.L., Schulein, B.J., and Wang, Z.X., 1992. Sedimentary Record and Climatic Implications of Recurrent Deformation in the Tian-Shan - Evidence from Mesozoic Strata of the North Tarim, South Junggar, and Turpan Basins, Northwest China. *Geol. Soc. Am. Bull.*, **104**, 53-79.

Hendrix, M.S., Dumitru, T.A. and Graham, S.A., 1994. Late Oligocene Early Miocene Unroofing in the Chinese Tien-Shan - an Early Effect of the India-Asia Collision. *Geology*, **22**, 487-490.

Hendrix, M.S., 2000. Evolution of mesozoic sandstone compositions, southern Junggar, northern Tarim, and western Turpan basins, northwest China: A detrital record of the ancestral Tian Shan. *J. Sed. Res.*, **70**, 520-532.

Huang, B. and Li, J., 2007. Sporopollen assemblages from the Xishanyao and Toutunhe formations at the Honggou section of the manasi river, xinjiang and their stratigraphical significance. *Acta Micropaleontologica Sinica*, **24**, 170-193.

Jolivet, M., Ritz, J.F., Vassalo, R., Larroque, C., Braucher, R., Todbileg, M., Chauvet, A., Sue, C., Arnaud, N., de Vicente, R., Arzhanikova, A. and Arzhanikova, S., 2007. Mongolian summits: An uplifted, flat, old but still preserved erosion surface. *Geology*, **35**, 871-874.

Jolivet, M., Dominguez J., Charreau J., Chen, Y., Farley, K.A., Li, Y.A. and Wang, Q.C., 2010. Mesozoic and Cenozoic tectonic history of the Central Chinese Tian Shan: Reactivated tectonic structures and active deformation. *Tectonics*, **29**, TC6019, doi:10.1029/2010TC002712.

Laurent-Charvet S., Charvet, J., Shu, L.S., Ma, R.S. and Lu, H.F., 2002. Late Paleozoic collisional strike-slip deformations in Tianshan and Altay, eastern Xinjiang, NW China. *Terra Nova*, **14**, 249-256.

Li Z., Zhang L., Qian C., Wang Y. and Bai G., 1978. Regional geological survey report of Geological map 1:200000, Shichang sheet. China Ministry of Geology and Mineral Resource, Beijing.

Li, Z., Song, W.J., Peng, S.T., Wang, D.X. and Zhang, Z.P., 2004. Mesozoic-Cenozoic tectonic relationships between the Kuqa subbasin and Tian Shan, northwest China: constraints from depositional records. *Sed. Geol.*, **172**, 223-249.

Liu, Z., 1990. Sporo-pollen assemblage from Middle Jurassic Xishanyao Formation of Shawan, Xinjiang, China. *Acta Palaeontologica Sinica*, **29**, 63-82.

Lu Y.Z. and Deng S.W., 2005. Triassic-Jurassic Sporopollen Assemblages on the Southern Margin of the Junggar Basin, Xinjiang and the T-J Boundary. *Acta Geologica Sinica*, **79**, 15-28.

352 Martinod, J., and Davy, P., 1992. Periodic instabilities during compression of the lithosphere
353 1. Deformation modes from an analytical perturbation method. *J. Geophys. Res.*, **92**, 1999–
354 2014.

355 Martinod, J. and Davy, P., 1994. Periodic instabilities during compression of the lithosphere 2.
356 Analogue experiments. *J. Geophys. Res.*, **99**, 12057–12069.

357 Métivier, F. and Gaudemer, Y., 1997. Mass transfer between eastern Tien Shan and adjacent
358 basins (central Asia): Constraints on regional tectonics and topography. *Geophys. J. Int.*, **128**,
359 1-17.

360 Sengör, A.M.C., Natal'in, B.A., Burtman, V.S., 1993. Evolution of the Altaid tectonic collage
361 and Paleozoic crust growth in Eurasia. *Nature*, **364**, 299-307.

362 Sobel, E.R. and Dumitru, T.A., 1997. Thrusting and exhumation around the margins of the
363 western Tarim basin during the India-Asia collision. *J. Geophys. Res.*, **102**, 5043-5063.

364 Tapponnier, P. and Molnar, P., 1977. Active Faulting and Tectonics in China. *J. Geophys.*
365 *Res.*, **82**, 2905-2930.

366 Wang, B. Chen, Y., Zhan, S., Shu, L.S., Faure, M., Cluzel, D., Charvet, J. and Laurent-
367 Charvet, S., 2007. Primary Carboniferous and Permian paleomagnetic results from the Yili
368 Block (NW China) and their implications on the geodynamic evolution of Chinese Tian Shan
369 Belt. *Earth Planet. Sci. Lett.*, **263**, 288-308.

370 Wang, Q. C., Li S. J. and Du z. L., 2009. Differential uplift of the Chinese Tian Shan since the
371 Cretaceous: constraints from sedimentary petrography and apatite fission-track dating. *Int. J.*
372 *Earth Sci.*, **98**, 1341-1363.

Wang, X.W., Wang, X.W., Liu, J.P., Liu, J.P. and Ma, Y.S., 2005. Analysis of the fold-thrust zone in the southern Junggar Basin , north western China. *Earth Science Frontiers*, **12**, 411-421.

Wang, Z., Wu, J., Lu, X., Liu, C., and Zhang, J., 1990, Polycyclic tectonic evolution and metallogeny of the Tian Shan mountains. Beijing, Science Press.

Windley, B.F., Allen, M.B., Zhang, C., Zhang, C., Zhao, Z.Y. and Wang, G.R., 1990. Paleozoic accretion and Cenozoic redeformation of the Chinese Tien Shan range, Central Asia. *Geology*, **18**, 128-131.

XBGMR-WUSU, 1973, Bureau of Geological and Mineral Resources of Xinjiang Uygur Autonomous Region, Geological map of Wusu Region, Scale 1:200.000, China Ministry of Geology and Mineral Resource, Beijing.

XBGMR-HOUXIA, 1977, Bureau of Geological and Mineral Resources of Xinjiang Uygur Autonomous Region, Geological map of Houxia Region, Scale 1:200.000, China Ministry of Geology and Mineral Resource, Beijing.

XBGMR-SHICHANG, 1978, Bureau of Geological and Mineral Resources of Xinjiang Uygur Autonomous Region, Geological map of Shichang Region, Scale 1:200.000, China Ministry of Geology and Mineral Resource, Beijing.

XBGMR, 1993, Regional geology of Xinjiang Uygur autonomy region.– Geological Memoirs, Ser. 1, No. 32, Map Scale 1: 1.500.000, Geological Publishing House, Beijing.

Yang, J., and Sun, S., 1982. The discovery of Early and Middle Jurassic megaspores from the Junggar Basin, Xinjiang, and their stratigraphic significance. *Acta Geologica Sinica*, **4**, 375–379.

395 Yang, J.L, Wang Q.F. and Lu H.N., 2005, Discovery of cretaceous and Paleocene charophyte
396 floras from well Hu-2 in the southern edge of Junggar basin. Acta Micropalaeontologica
397 Sinica, **22**, 251-268.

398 ***Figure captions***

399 Fig. 1 Simplified geological map of the northern Tian Shan from Wusu to Urumqi areas.
400 Mesozoic is most exposed in the southernmost parts of the Junggar basin along the adjacent
401 Tian Shan range, particularly to the East (Urumqi area). 'He' indicates river in Chinese
402 (modified after XBGMR, 1993).

403 Fig. 2 Synthetic and representative stratigraphic log made in the Manasi He area, northern
404 Tian Shan piedmont, where Cenozoic have been widely eroded (modified after Hendrix et al.,
405 1992).

406 Fig. 3 Landscape pictures of representative features of the Mesozoic sedimentary series (see
407 locations on Fig.1) (a) Coarse-grained conglomerate of lowermost Jurassic forming prominent
408 bars in the landscape (southern Qingshui He area); (b) Uppermost Jurassic coarse-grained
409 breccias (Kalaza Fm. - J_{3k}) unconformably overlying the Upper Jurassic Qigu formation (J_{3q} ;
410 Hutubi He area); (c) Close-up view of the Uppermost Jurassic Kalaza Fm. breccias (west to
411 Hutubi He area). Note the angular shape of the clasts (locally exceeding 50 cm) and the clast-
412 supported character of the coarser levels.

413 Fig. 4 Structural and sedimentological observations in the Houxia area. (a) Simplified
414 geological map with some field structural measurements (modified after XBGMR, 1977), (b)
415 detailed geological cross-section across the northern limb of the syncline structure (see
416 location on Fig. 4a), (c) Close-up view of the Lower Jurassic breccias including
417 Carboniferous basement angular clasts (see location on Fig. 4b), (d) picture of the steep
418 bedding of Jurassic layers close to the southward thrust (see location on Fig. 4b).

419 Fig. 5 (a) Simplified geological map of the Hutubi He area (modified after XBGMR, 1978,
420 1993) with few structural measurements from field work. 'A' indicates location where Middle

421 Jurassic deposits directly and unconformity lie onto Carboniferous basement without Triassic
422 or Lower Jurassic, (b) Geological cross-section along the Hutubi He constrained by field data,
423 seismic profile (after Wang et al., 2005) and nearby drill wells W1 and W1'. Location of the
424 section is indicated on Fig. 5a. Extension of the available seismic profile is indicated on the
425 section.

426 Fig. 6 Examples of onlap structures of the Jurassic sediments over the Paleozoic basement
427 units. (a) Picture and interpretation field sketch of the southern part of the Hutubi He (see
428 location on Fig. 5a): note the overall southward onlap of the Jurassic sediments over the
429 folded basement. To the north, a basement block is back thrusted over the sediments (see Fig.
430 5b), (b) Picture and interpretation field sketch of a small valley, west of the Hutubi He (see
431 location on Fig. 5a): meso-scale basement relief covered by Jurassic sandstones as evidenced
432 by onlaps over a steep inherited ~150 m high basement paleorelief (scarp). Basement rocks
433 are deformed with a large inclined Paleozoic fold.

434 Fig. 7 Structural and sedimentological observations in the Wusu area. (a) Simplified
435 geological map (modified after XBGMR, 1973) with few structural measurements. (b)
436 Geological cross-section constrained by field data, seismic profile and drill well W2 (see Fig.
437 7a for location). (c) Picture and corresponding field sketch interpretation of the
438 unconformable contact between Jurassic layers and the Carboniferous basement (see Fig. 7a
439 for location).

440 Fig. 8 Sketch views of the paleogeographic evolution of the northern piedmont of Tian Shan
441 during Early, Middle and Upper Jurassic/Cretaceous boundary. Main observations that
442 constrain this study are localized on the drawings as: A for Fig. 3a; B for Fig. 4c (lower
443 Jurassic sedimentary breccias); C for Fig. 6a (onlap covering of Paleozoic basement rocks by

444 Jurassic sandstones) and D for Figs. 3b and 3c (thick Kalaza Fm. breccias with angular

445 discordance at the base).

The Mesozoic paleorelief of the northern Tian Shan (China)

Ke CHEN[1,2], Charles GUMIAUX[1], Romain AUGIER[1], Yan CHEN[1], Qingchen WANG[2] , Wei LIN[2] , Shengli WANG[3] ,

1. Institut des Sciences de la Terre d'Orléans (ISTO), Université d'Orléans, CNRS: UMR6113, Université François Rabelais - Tours, - INSU, Campus Géosciences, 1A rue de la Férollerie, 45071 Orléans cedex 2, France

2. State Key Laboratory of Lithospheric Evolution, Institute of Geology and Geophysics, Chinese Academy of Sciences, P.O. 9825, Beijing 100029, China

3. Department of Earth Sciences, Nanjing University, 210093, Nanjing, China

Abstract

The Tian Shan range offers a natural laboratory to study orogenic processes. Most of the previous studies focused on either the Paleozoic evolution of the range or its Cenozoic intracontinental evolution linked with the India-Asia collision. In this study, detailed field investigations on the relationship between sedimentary cover and basement constrain the Mesozoic evolution of the northern Tian Shan. Sedimentological observations argue for limited transport distance for Lower and Uppermost Jurassic deposits. Geological sections presented in this paper show that, in preserved locations, Triassic to Jurassic sedimentary series present a continuous onlap type sedimentary unconformity on the top of the basement. At different scales, observations clearly evidence the existence of a major paleorelief during Mesozoic. According to the present study, the current Tian Shan range topography and the associated movements along its northern front structures cannot be considered as the consequence of Cenozoic reactivation alone.

Keywords

Tian Shan, paleorelief, Mesozoic, regional onlap, reactivation, India-Asia collision.

Introduction

The modern Tian Shan is one of the major mountain ranges in Central Asia. The current structure of Tian Shan mainly results from a combination of two main tectonic events: i) subductions, arc-accretions and continental collision during Paleozoic (e.g. Carroll et al., 1990; Wang et al., 1990; Windley et al., 1990; Sengör et al. 1993; Carroll et al., 1995; Gao et al., 1998; Laurent-Charvet et al., 2002; Charvet et al., 2007; Wang et al., 2007) and ii) intracontinental reactivation linked to the India-Asia collision, during Cenozoic (e.g. Tapponnier and Molnar, 1977; Avouac et al., 1993). At first order, the modern Tian Shan corresponds to a raised ~east-west trending Paleozoic 'basement' range, flanked by two closed intracontinental basins whose infill is a particularly accurate record for both tectonic and climate evolutions (Fig. 1). The present-day high topography of Tian Shan, with a mean altitude of ~2500 m and summits of more than 7000 m, is traditionally related to the latest intracontinental deformation of the range (e.g. Tapponnier and Molnar, 1977; Avouac et al., 1993; Burchfiel et al., 1999). Age constraints for the onset of this intracontinental reactivation range from 10 to 24 Ma (e.g. Avouac et al., 1993; Hendrix et al., 1994; Abdrakhmatov et al., 1996; Métivier and Gaudemer, 1997; Sobel et al., 1997; Dumitru et al., 2001; Charreau et al., 2009). In spite of relative age discrepancies (mostly related to the method applied), all ages estimated for the deformation and the associated relief erosion suggest that the mountain range reactivation and relief creation began during Early Miocene at oldest.

However, recent Fission-track analyses suggest that uplifting may have existed well before the onset of the Tertiary reactivation through Tian Shan, with exhumation ages such as 160-120 Ma in central Tian Shan, 200-250 Ma detritus cooling age in the Manas River valley (Dumitru et al., 2001; Jolivet et al., 2010) or 140-120 Ma from Bayanbulak intracontinental basin, in the southern Tian Shan (Wang et al., 2009). Moreover, Triassic to Cretaceous sediments are composed of thick continental series characterized by massive coarse-grained

formations within both basins, suggesting rather high erosion rate at that time (Hendrix, 2000; Carroll et al., 2010).

This study considers the Mesozoic tectonic and morphologic evolution of Tian Shan through field structural and sedimentological analyses of Mesozoic deposits. It focuses on the northern piedmont of the range, along a ~280 km west-east trending segment (Fig. 1). Thanks to deep incisions of seasonal rivers, contacts between Paleozoic basement and Mesozoic-Cenozoic sedimentary cover are particularly well exposed along several north-south trending sections in this region (Fig. 1). Such new constraints on Mesozoic evolution of the Tian Shan area would lead to reconsider the contribution of Cenozoic tectonics in the modern mountain range building as well as to better quantify the net shortening amount during that period.

Stratigraphy of the Mesozoic sediments within the study area

Sedimentary series can be extensively observed and have already been studied within the Junggar basin, as summarized below (Figs. 1 and 2; Hendrix et al., 1992 and references therein; XBGMR, 1993). Basement units of the north Tian Shan mainly consist of Paleozoic volcanic and sedimentary rocks. From bottom to top, the entire Mesozoic series is composed of ~5 km thick continental clastic deposits highlighting high sedimentation/preservation rates (Fig. 2). Thanks to numerous studies aimed at oil and gas exploration and to 1:200.000 mapping projects hold in this area, ages of the Mesozoic sequences were mainly constrained by floral and sporopollen assemblage analyses (Li et al., 1978; Yang et al., 1982; Liu, 1990; XBGMR, 1993; Lu and Deng, 2005; Yang et al., 2005; Huang and Li, 2007). In the study area, the Triassic series are mostly missing along the piedmont though locally exposed (Fig. 1). Where it crops out, Triassic displays alluvial sandstones and conglomerates intercalated within and silty mudstones (red-beds). At the scale of the northern Tian Shan piedmont, Lowermost Jurassic layers indicate a change in the sedimentation as they consist in thick and

coarse conglomeratic deposits, as exposed in the south of Qingshui He (Fig. 3a). Thickness of Lower Jurassic reaches 1000 m over the area extending from Manasi to Urumqi, and decreases westwardly and eastwardly. Sediments become progressively finer upward, grading into ~3 km thick series of Lower/Middle Jurassic gray sandstones, silty shales (Fig. 2). Middle Jurassic sandstones and mudstones locally contain coal-rich layers consistent with a lacustrine depositional facies (Hendrix et al., 1992). Upper Jurassic comprises typical fine-grained red beds where conglomerates remain scarce. The transition from Jurassic to Cretaceous series is marked by up to 800 m thick sedimentary breccias (Kalaza formation – J3k; Fig. 3b) made of coarse-grained angular clasts (Fig. 3c). It rapidly dies laterally and grades to sandstones within the Junggar basin itself (XBGMR, 1978; 1993). The marked unconformity between the Kalaza formation and the underlying finer-grained Upper Jurassic red beds (Fig. 3b) suggests a short transport distance of material before deposition and nearby relief uplifting.

In this study, Mesozoic sediments have also been extensively observed within internal parts of the range, and more particularly in the eastern part of the studied area (Fig. 1). Triassic to Jurassic sediments are encountered on top of the Paleozoic basement units, at rather high altitudes (2000 to 3000 m) in comparison with the mean altitude of the foreland fold-and-thrust belts (1000 to 1500 m high). In the Houxia valley for instance – 65 km SSW of Urumqi – a Lower to Upper Jurassic continuous sedimentary series is preserved in a syncline structure (Fig. 4a). According to the geological map (Fig. 4a; XBGMR, 1977), Lower Jurassic formations – i.e. Shangonghe Fm. to the northwest and Lowermost Jurassic Badaowan Fm. to the east – directly overlie on top of Carboniferous basement units, without intercalated Triassic sediments. Besides, south and north verging thrusts developed along parts of the northern and southern limbs of the fold, respectively (Fig. 4a). A section made across the north limb of the syncline displays continuous Lower to Middle Jurassic series with

no fault contact observed (Fig. 4b). From south to north, bedding planes progressively straighten up from ~30° south dipping to vertical, and even overturned just below the south verging thrust (Figs. 4a ,4b and 4d). From a sedimentological point of view, the upper and main part of Jurassic series is made of fine-grained sandstones and mudstones while the lowermost deposits of the series is characterized by intercalations of coarse-grained sedimentary breccias mostly made of highly angular clasts of Carboniferous tuffaceous sandstones (Fig. 4c). Local abundance of these breccias and the common lithological nature of the clasts with the adjacent basement unit strongly suggest a very short transport distance.

Structural analysis of the Mesozoic basal contact

Deformation of the northern Tian Shan has already been studied through the structural analysis of sedimentary series, within the Cenozoic foreland basin (e.g. Avouac et al., 1993; Deng et al., 1996; Burchfiel et al., 1999). This part focuses on the basal contact of the Mesozoic sediments, in the northern "front" area of Tian Shan.

As shown on the map (Fig. 1), some parts of the piedmont display northward thrusts that mark out the boundary in between the Paleozoic uplifted basement units and relatively subsiding proximal foreland basin. Yet, as described above, Mesozoic series are not solely restricted to the piedmont fold-and-thrust belts but are also well preserved on top of the basement units, within the range (Fig. 1). Then, some other segments of the piedmont display perfectly continuous Mesozoic sedimentary series from basin until internal and higher parts of the range, without being strained by any faulting or folding in the range front area (Fig. 1). Structural analysis of such unstrained basal contact of Mesozoic series is presented for two of the sections constructed from field work combined with available seismic profiles and drill-holes data: the Hutubi He and the Wusu sections (Fig. 1).

120 At first order, to the north of the Hutubi He area, Triassic to Neogene sedimentary
121 series form a rather simple monocline structure, dipping 15-20° to the north (Fig. 5a). The
122 southernmost fold-and-thrust belt is composed of one gentle upright anticline and associated
123 syncline with only very limited thrusts developed along the hinge of the fold (Fig. 5a). This
124 belt can be regarded as a fault-propagation fold structure according to the available seismic
125 profile (Wang et al., 2005; Fig. 5b). Further south, entering within the interior parts of the
126 range, sub-horizontal Lower Jurassic strata lie on top of the Carboniferous units (Fig. 5b).
127 While basement is strongly deformed, as evidenced by sub-vertical cleavage, its sedimentary
128 cover is only gently folded as illustrated on the geological map, few kilometers west of the
129 river (Fig. 5a; XBGMR, 1978, 1993). No décollement structure has been observed between
130 the basement top and the sedimentary cover. Besides, a southward backthrust of basement
131 rocks above sediments can be observed to the south of the section, but the net slip must be
132 limited as it rapidly dies out, the fault laterally evolving to a fold toward the west (Fig. 5a).
133 Unconformity of the basal contact of Mesozoic sediments on top of basement units is
134 observed in the southernmost part of the section (Figs. 5a and 6a). As a whole, the successive
135 sub-horizontal and monocline segments define a hinge fold at regional scale (Fig. 5b).
136 Nevertheless, while ~900 m thick of Triassic sediments have been drilled along the W1 well
137 in the basin (Fig. 5b), no Triassic series have been observed further south in the range, in the
138 section area (Fig. 5a). Indeed, Lowermost to Middle Jurassic levels have been observed and
139 mapped directly on top of the basement units (Fig. 5a; XBGMR, 1978, 1993). Similarly to the
140 Houxia area, basal contact of the Mesozoic series suggests its onlap deposit, from basin to
141 range, at least during Triassic and Lower-Middle Jurassic.

142 More local-scale evidences for onlap sedimentation can also be observed in the Hutubi
143 He area. First, to the south end of the section, Lower Jurassic strata display a kilometer scale
144 onlap type structure on top of basement units, i.e. with younger sediments progressively

covering basement, from north to south (Figs. 5a and 6a). Second, ~10 km west of the Hutubi River, subhorizontal layers of the Lower Jurassic formation, which can be continuously followed in few kilometers in this small valley, structurally onlap on the deformed Paleozoic basement units (Fig. 6b). There, stratification planes are markedly oblique with the top of the Paleozoic units and no deformation has been observed along this contact. In the landscape, younger Jurassic sediments progressively extend to the south, on top of the Carboniferous units. Sediments progressively overlie and cover a ~150 m high step of the basement top which implies that a significant relief existed during Jurassic sediments deposition.

To the north of the Wusu section, first-order structure of the Mesozoic-Cenozoic series displays a 40-45° north dipping monocline (Figs. 7a and 7b). To the south, bedding is sub-horizontal and structure of the sedimentary series is marked by a large hinge fold. As drawn on the geological map, thrust faults are observed at the surface, but seismic data show that they do not extend downward into the Mesozoic series (Fig. 7b; *suppl. material*), which is compatible with the limited throw produced by these faults as deduced from map data analysis (Fig. 7a). While ~400 m of Triassic sediments have been found in a drilled well in the basin, close to this section (see W2 on Fig. 7a), Triassic series becomes much thinner to the south and Jurassic sandstones, sometimes, directly lie on top of the Carboniferous rocks with an erosional undeformed contact (Fig. 7c; XBGMR, 1973).

Discussion and conclusions

In parallel to rather classical view of frontal thrust systems, this study highlights that the northern piedmont of Tian Shan also displays segments where Mesozoic series are preserved unconformably onto the basement with onlap-type relationships. Such features are pointed out along two distant cross-sections and have also been clearly shown at outcrop-scale. Sedimentary breccias, showing very limited transport distances, have been found within

Lower Jurassic sediments of the internal parts of the range. Whatever the scale, all these observations clearly show the existence of proximal relief when Triassic/Jurassic sediments were deposited. Our field observations are consistent with previously published sedimentological data – paleocurrent measurements, heavy mineral composition, sedimentological source analyses – in the Junggar and Tarim basins which suggest that Tian Shan could already have existed as a "positive" geomorphologic feature during Mesozoic times (Hendrix et al., 1992, Graham et al., 1993; Hendrix, 2000; Li et al., 2004).

In the field, the local-scale observation of onlap sedimentary architecture reveals that the paleo-altitude difference can reach 100-150 m in a hectometer horizontal distance, which highlights local steep slopes (cf. Fig. 6b). Together with the sedimentological observations in the Houxia valley, this suggests that small-scale ridges with intercalated intra-mountainous basins have probably existed during Mesozoic (Fig. 8a).

Drill wells W1 and W1' (Figs. 4a and 4b) display ~1200 m of Lower Jurassic sediments (e.g. Badaowan and Shangonghe Fm., Fig. 2). A comparable thickness for Lower Jurassic has also been observed in the Manas area, 50 km west of the Hutubi section (Fig. 2; Hendrix et al., 1992). Following the geological maps (XBGMR; 1978, 1993), Middle Jurassic series directly lie unconformably onto the Carboniferous basement, without Triassic and Lower Jurassic sediments in the southern part of the Hutubi River (see location A in Fig. 4a). The thickness difference of Jurassic sediments reaches ~1200 m between the location A and the drill well location, for a horizontal distance of about 50 km (Fig. 4a). Such thickness difference may result from subsidence mechanisms. However, whatever the scale considered in this study, Triassic and mostly Jurassic series, up to the late Jurassic Kalaza formation deposit, display parallel bedding with no growth strata observed (Figs. 5b, 6 and 7b). Such feature shows that, at the scale of the studied area, significant vertical differential movements may have hardly occurred during Triassic to Upper Jurassic sedimentation. In addition, as

described above, Jurassic strata often overlie directly on Carboniferous by onlap, without fault or syn-sedimentary deformations. Seismic profiles across the southern margin of the Junggar basin do not display major fault that could have controlled sedimentation for the Early Jurassic period (Allen et al., 1991; Wang et al., 2005). No evidence for structural control on local subsidence could thus be argued here. At larger scale, flexure – either thermal or tectonic – could also have controlled the subsidence for Mesozoic series accumulation.

If considering thermal control, the latest regional tectono-magmatic event occurring before Mesozoic in the Central Tian Shan area ended during early Permian (see compilation by Han et al., 1999), which is about 100 Ma earlier than Jurassic sedimentation. Therefore, according to Hendrix et al. (1992), it seems that thermal driving mechanism may only play a weak role for the Early and Middle Jurassic sedimentation. If considering tectonic control, compressional flexure may also be hard to explain as, for comparable vertical differential movements, buckling of a stable continental lithosphere would result in much larger wavelength (200-300 km) than observed in this study (~50 km) as shown by mechanical modelling (Martinod and Davy, 1992, 1994; Burov et al., 1993; Cloetingh et al., 1999).

At the scale of the present study, Jurassic sedimentation seems hardly controlled by either tectonic or thermal subsidence across northern Tian Shan. Accordingly, the 1200-1300 m thickness difference may be mainly produced by infilling of a long-lasting remnant relief of, at least, 1200-1300 m high at that period (i.e. from Triassic/Lowermost Jurassic; Fig. 8a). During Middle Jurassic, finer-grained sediments were conformably deposited on top of the Lower Jurassic strata within the basin, and were deposited onlap on the Paleozoic basement toward the range (Figs. 5a and 8b). Middle Jurassic sediments of the Xishanyao and Toutunhe formations extend to a larger area with respect to the Lower Jurassic and, as a whole, the paleorelief lateral extension was certainly less important during Middle Jurassic than during Triassic/Early Jurassic (Fig. 8b). During latest Jurassic to Early Cretaceous, thick

breccias were deposited onto the Middle Jurassic sediments through an angular unconformity (*cf.* Kalaza Fm.). These breccias are restricted to the front of the modern Tian Shan and change rapidly to finer-grained deposits in lateral equivalents. This configuration is reminiscent of the general architecture of current fans deposited along the modern Tian Shan range that originate from the present day high relief to the south, but show limited northward transport of sediments (Fig. 8c). In turn, location of the main morphological northern front of the paleo- Tian Shan, during Latest Jurassic to Early Cretaceous, would approximately coincide with the one of the current range front (Fig. 5). The uplift documented by these coarse-grained sedimentary breccias is also recorded by AFT chronology studies; Fission-track modeling indicates a ca. 160 and 120 Ma cooling age along a Dushanzi-Kuqa corridor, in the mountain interior (Dumitru et al., 2001; Jolivet et al., 2010). Apatite sampled from Bayanbulak area yields the earliest cooling ages of Early Cretaceous (Dumitru et al., 2001; Wang et al. 2009).

Because no major tectonic event occurred in the Northern Tian Shan during Mesozoic times (e.g. De Grave et al., 2007), the Paleozoic subduction-collision orogeny (Gao et al., 1998; Laurent-Charvet et al., 2002; Charvet et al., 2007) appears as the most probable origin of the Mesozoic paleorelief above described. In such case, the Tian Shan would persist as remnant relieves for several tens of Ma after the end of the orogenic events which are progressively and unconformably overlain by Triassic and then Jurassic sedimentation (e.g. onlap structures, mesoscale paleorelief infilling). This scenario implies extremely low erosion rates to allow the preservation of a significant relief; such feature has already been reported for other regions of Central Asia from thermochronological (AFT) and field data analyses (Jolivet et al., 2007). In parallel, Central Asia Mesozoic tectonic history is marked by the polyphased Cimmerian orogeny in Tibet area (e.g. Hendrix et al., 1992; Sobel and Dumitru, 1997; De Grave et al., 2007). Low amplitude, far-field effects can thus be recognized in the

Mesozoic northern Tian Shan: one early collision stage – Qiantang/Kunlun blocks during Late Triassic/Middle Jurassic – would correspond to the drastic coarsening of the Lower Jurassic sedimentation. In turn, a later collision stage – Lhasa/Qiantang blocks during Late Jurassic/Early Cretaceous – well corresponds to the deposits of the thick and coarse breccias of the Kalaza Fm. at that time. In this case, a tectonic origin of the relief rejuvenation is attested by a major angular unconformity observed regionally.

As unambiguously demonstrated, the physiography of the modern Tian Shan dominantly results from the recent tectonic evolution of the area (e.g. Tapponnier and Molnar, 1977; Avouac et al., 1993; Métivier and Gaudemer, 1997; Charreau et al., 2009). However, this study put forward that the current Tian Shan topography can probably not be considered as the consequence of the Cenozoic intracontinental reactivation alone, but as a combination of the Cenozoic deformations superimposed on a reminiscent Mesozoic paleo-range. These new results question on the amplitude of the movements that could be estimated along the northern front structures during Cenozoic intracontinental reactivation.

Acknowledgements

Field and laboratory work in the present study are financially supported by Chinese National 973 Program (2009CB825008) and Chinese National S&T Major Project 2011ZX05008. Prof. A.R. Caroll, Dr. J. Charreau, and an anonymous reviewer are warmly thanked for their constructive reviews. We are also grateful for the help by Prof. Carlo Doglioni (*Editor*) and Prof. Gerhard Wörner (*Associate Editor*). Discussions on seismic profiles' interpretation with Dr. Y. Branquet have also been greatly appreciated. The first author benefices a Ph.D scholarship from French Embassy in Beijing and IGGCAS.

References

Abdrakhmatov, K.Y., Aldazhanov, S.A., Hager, B.H., Hamburger, M.W., Herring, T.A., Kalabaev, K.B., Makarov, V.I., Molnar, P., Panasyuk, S.V., Prilepin, M.T., Reilinger, R.E., Sadybakasov, I.S., Souter, B.J., Trapeznikov, Y.A., Tsurkov, V.Y. and Zubovich, A.V., 1996. Relatively recent construction of the Tien Shan inferred from GPS measurements of present-day crustal deformation rates. *Nature*, **384**, 450-453.

Allen, M.B., Windley, B.F., Zhang, C., Zhao, Z.Y. and Wang, G.R., 1991. Basin Evolution within and Adjacent to the Tien-Shan Range, NW China. *J. Geol. Soc. London*, **148**, 369-378.

Avouac, J.P., Tapponnier, P., Bai, M., You, H. and Wang, G., 1993. Active Thrusting and Folding Along the Northern Tien-Shan and Late Cenozoic Rotation of the Tarim Relative to Dzungaria and Kazakhstan. *J. Geophys. Res.*, **98**, 6755-6804.

Burchfiel, B.C., Brown, E.T., Deng, Q.D., Feng, X.Y., Li, J., Molnar, P., Shi, J.B., Wu, Z.M. and You, H.C., 1999. Crustal shortening on the margins of the Tien Shan, Xinjiang, China. *Int. Geol. Rev.*, **41**, 665-700.

Burov, E.B., Lobkovsky, L.I., Cloetingh, S. and Nikishin, A.M., 1993. Continental lithosphere folding in Central Asia (Part II): constraints from gravity and topography. *Tectonophysics*, **226**, 73–87.

Carroll, A.R., Liang, Y., Graham, S.A., Xiao, X., Hendrix, M.S., Chu, J., and McKnight, C.L., 1990. Junggar basin, northwest China: Trapped late Paleozoic ocean. *Tectonophysics*, **181**, 1-14.

Carroll, A. R., Graham, S.A., Hendrix, M.S., Ying, D., and Zhou, D., 1995. Late Paleozoic tectonic amalgamation of northwestern China: sedimentary record of the northern Tarim, northwestern Turpan, and southern Junggar basins. *Geol. Soc. Am. Bull.*, **107**, 571-594.

Carroll, A.R., Graham, S.A. and Smith, M.E., 2010. Walled sedimentary basins of China. *Basin Res.*, **22**, 17-32.

Charreau, J., Chen, Y., Gilder, S., Barrier, L., Dominguez, S., Augier, R., Sen, S., Avouac, J.P., Gallaud, A., Graveleau, F. and Wang, Q.C., 2009. Neogene uplift of the Tian Shan Mountains observed in the magnetic record of the Jingou River section (northwest China). *Tectonics*, **28**, TC2008, doi:10.1029/2007TC002137.

Charvet, J., Shu, L.S. and Laurent-Charvet, S., 2007. Paleozoic structural and geodynamic evolution of eastern Tianshan (NW China): welding of the Tarim and Junggar plates. *Episodes*, **30**, 162-186.

Cloetingh, S., Burov, E. and Poliakov, A., 1999. Lithosphere folding: primary response to compression? (from central Asia to Paris basin). *Tectonics*, **18**, 1064–1083.

De Grave, J., Buslov, M.M. and Van den Haute, P., 2007. Distant effects of India–Eurasia convergence and Mesozoic intracontinental deformation in Central Asia: Constraints from apatite fission-track thermochronology. *J. Asian Earth Sc.,* **29,** 188-204.

Deng, Q.D., Zhang, P.Z., Xu, X.W., Yang, X.P., Peng, S.Z., and Feng, X.Y., 1996. Paleoseismology of the northern piedmont of Tianshan Mountains, northwestern China. *J. Geophys. Res.*, **101**, 5895-5920.

Dumitru, T.A., Zhou, D., Chang, E.Z., Graham, S.A., Hendrix, M.S., Sobel, E.R., and Caroll, A.R., 2001. Uplift, exhumation, and deformation in the Chinese Tian Shan. in: Paleozoic and

Mesozoic tectonic evolution of central Asia: From continental assembly to intracontinental deformation (Hendrix, M.S., and Davis,G.A., eds). *Geol. Soc. Am. Mem.*, **194**, 71–99.

Gao, J., Li, M.S., Xiao, X.C., Tang, Y.Q. and He, G.Q., 1998. Paleozoic tectonic evolution of the Tianshan Orogen, northwestern China. *Tectonophysics*, **287**, 213-231.

Graham, S.A., Hendrix, M.S., Wang, L.B. and Carroll, A.R., 1993. Collisional successor basins of western China Impact of tectonic inheritance on sand composition. *Geol. Soc. Am. Bull.*, **105**, 323-344.

Han B.F., He, G.Q. and Wang, S., 1999. Postcollisional mantle-derived magmatism, underplating and implications for basement of the Junggar Basin. *Sci. China. Ser. D*, **42**, 113-119.

Hendrix, M.S., Graham, S.A., Carroll, A.R., Sobel, E.R., Mcknight, C.L., Schulein, B.J., and Wang, Z.X., 1992. Sedimentary Record and Climatic Implications of Recurrent Deformation in the Tian-Shan - Evidence from Mesozoic Strata of the North Tarim, South Junggar, and Turpan Basins, Northwest China. *Geol. Soc. Am. Bull.*, **104**, 53-79.

Hendrix, M.S., Dumitru, T.A. and Graham, S.A., 1994. Late Oligocene Early Miocene Unroofing in the Chinese Tien-Shan - an Early Effect of the India-Asia Collision. *Geology*, **22**, 487-490.

Hendrix, M.S., 2000. Evolution of mesozoic sandstone compositions, southern Junggar, northern Tarim, and western Turpan basins, northwest China: A detrital record of the ancestral Tian Shan. *J. Sed. Res.*, **70**, 520-532.

Huang, B. and Li, J., 2007. Sporopollen assemblages from the Xishanyao and Toutunhe formations at the Honggou section of the manasi river, xinjiang and their stratigraphical significance. *Acta Micropaleontologica Sinica*, **24**, 170-193.

Jolivet, M., Ritz, J.F., Vassalo, R., Larroque, C., Braucher, R., Todbileg, M., Chauvet, A., Sue, C., Arnaud, N., de Vicente, R., Arzhanikova, A. and Arzhanikova, S., 2007. Mongolian summits: An uplifted, flat, old but still preserved erosion surface. *Geology*, **35**, 871-874.

Jolivet, M., Dominguez J., Charreau J., Chen, Y., Farley, K.A., Li, Y.A. and Wang, Q.C., 2010. Mesozoic and Cenozoic tectonic history of the Central Chinese Tian Shan: Reactivated tectonic structures and active deformation. *Tectonics*, **29**, TC6019, doi:10.1029/2010TC002712.

Laurent-Charvet S., Charvet, J., Shu, L.S., Ma, R.S. and Lu, H.F., 2002. Late Paleozoic collisional strike-slip deformations in Tianshan and Altay, eastern Xinjiang, NW China. *Terra Nova*, **14**, 249-256.

Li Z., Zhang L., Qian C., Wang Y. and Bai G., 1978. Regional geological survey report of Geological map 1:200000, Shichang sheet. China Ministry of Geology and Mineral Resource, Beijing.

Li, Z., Song, W.J., Peng, S.T., Wang, D.X. and Zhang, Z.P., 2004. Mesozoic-Cenozoic tectonic relationships between the Kuqa subbasin and Tian Shan, northwest China: constraints from depositional records. *Sed. Geol.*, **172**, 223-249.

Liu, Z., 1990. Sporo-pollen assemblage from Middle Jurassic Xishanyao Formation of Shawan, Xinjiang, China. *Acta Palaeontologica Sinica*, **29**, 63-82.

Lu Y.Z. and Deng S.W., 2005. Triassic-Jurassic Sporopollen Assemblages on the Southern Margin of the Junggar Basin, Xinjiang and the T-J Boundary. *Acta Geologica Sinica*, **79**, 15-28.

Martinod, J., and Davy, P., 1992. Periodic instabilities during compression of the lithosphere 1. Deformation modes from an analytical perturbation method. *J. Geophys. Res.*, **92**, 1999–2014.

Martinod, J. and Davy, P., 1994. Periodic instabilities during compression of the lithosphere 2. Analogue experiments. *J. Geophys. Res.*, **99**, 12057–12069.

Métivier, F. and Gaudemer, Y., 1997. Mass transfer between eastern Tien Shan and adjacent basins (central Asia): Constraints on regional tectonics and topography. *Geophys. J. Int.*, **128**, 1-17.

Sengör, A.M.C., Natal'in, B.A., Burtman, V.S., 1993. Evolution of the Altaid tectonic collage and Paleozoic crust growth in Eurasia. *Nature*, **364**, 299-307.

Sobel, E.R. and Dumitru, T.A., 1997. Thrusting and exhumation around the margins of the western Tarim basin during the India-Asia collision. *J. Geophys. Res.*, **102**, 5043-5063.

Tapponnier, P. and Molnar, P., 1977. Active Faulting and Tectonics in China. *J. Geophys. Res.*, **82**, 2905-2930.

Wang, B. Chen, Y., Zhan, S., Shu, L.S., Faure, M., Cluzel, D., Charvet, J. and Laurent-Charvet, S., 2007. Primary Carboniferous and Permian paleomagnetic results from the Yili Block (NW China) and their implications on the geodynamic evolution of Chinese Tian Shan Belt. *Earth Planet. Sci. Lett.*, **263**, 288-308.

Wang, Q. C., Li S. J. and Du z. L., 2009. Differential uplift of the Chinese Tian Shan since the Cretaceous: constraints from sedimentary petrography and apatite fission-track dating. *Int. J. Earth Sci.*, **98**, 1341-1363.

373 Wang, X.W., Wang, X.W., Liu, J.P., Liu, J.P. and Ma, Y.S., 2005. Analysis of the fold-thrust
374 zone in the southern Junggar Basin , north western China. *Earth Science Frontiers*, **12**, 411-
375 421.

376 Wang, Z., Wu, J., Lu, X., Liu, C., and Zhang, J., 1990, Polycyclic tectonic evolution and
377 metallogeny of the Tian Shan mountains. Beijing, Science Press.

378 Windley, B.F., Allen, M.B., Zhang, C., Zhang, C., Zhao, Z.Y. and Wang, G.R., 1990.
379 Paleozoic accretion and Cenozoic redeformation of the Chinese Tien Shan range, Central Asia.
380 *Geology*, **18**, 128-131.

381 XBGMR-WUSU, 1973, Bureau of Geological and Mineral Resources of Xinjiang Uygur
382 Autonomous Region, Geological map of Wusu Region, Scale 1:200.000, China Ministry of
383 Geology and Mineral Resource, Beijing.

384 XBGMR-HOUXIA, 1977, Bureau of Geological and Mineral Resources of Xinjiang Uygur
385 Autonomous Region, Geological map of Houxia Region, Scale 1:200.000, China Ministry of
386 Geology and Mineral Resource, Beijing.

387 XBGMR-SHICHANG, 1978, Bureau of Geological and Mineral Resources of Xinjiang
388 Uygur Autonomous Region, Geological map of Shichang Region, Scale 1:200.000, China
389 Ministry of Geology and Mineral Resource, Beijing.

390 XBGMR, 1993, Regional geology of Xinjiang Uygur autonomy region.– Geological Memoirs,
391 Ser. 1, No. 32, Map Scale 1: 1.500.000, Geological Publishing House, Beijing.
392 Yang, J., and Sun, S., 1982. The discovery of Early and Middle Jurassic megaspores from the
393 Junggar Basin, Xinjiang, and their stratigraphic significance. *Acta Geologica Sinica*, **4**, 375–
394 379.

395 Yang, J.L, Wang Q.F. and Lu H.N., 2005, Discovery of cretaceous and Paleocene charophyte
396 floras from well Hu-2 in the southern edge of Junggar basin. Acta Micropalaeontologica
397 Sinica, **22**, 251-268.

398 ***Figure captions***

399 Fig. 1 Simplified geological map of the northern Tian Shan from Wusu to Urumqi areas.
400 Mesozoic is most exposed in the southernmost parts of the Junggar basin along the adjacent
401 Tian Shan range, particularly to the East (Urumqi area). 'He' indicates river in Chinese
402 (modified after XBGMR, 1993).

403 Fig. 2 Synthetic and representative stratigraphic log made in the Manasi He area, northern
404 Tian Shan piedmont, where Cenozoic have been widely eroded (modified after Hendrix et al.,
405 1992).

406 Fig. 3 Landscape pictures of representative features of the Mesozoic sedimentary series (see
407 locations on Fig.1) (a) Coarse-grained conglomerate of lowermost Jurassic forming prominent
408 bars in the landscape (southern Qingshui He area); (b) Uppermost Jurassic coarse-grained
409 breccias (Kalaza Fm. - J_{3k}) unconformably overlying the Upper Jurassic Qigu formation (J_{3q} ;
410 Hutubi He area); (c) Close-up view of the Uppermost Jurassic Kalaza Fm. breccias (west to
411 Hutubi He area). Note the angular shape of the clasts (locally exceeding 50 cm) and the clast-
412 supported character of the coarser levels.

413 Fig. 4 Structural and sedimentological observations in the Houxia area. (a) Simplified
414 geological map with some field structural measurements (modified after XBGMR, 1977), (b)
415 detailed geological cross-section across the northern limb of the syncline structure (see
416 location on Fig. 4a), (c) Close-up view of the Lower Jurassic breccias including
417 Carboniferous basement angular clasts (see location on Fig. 4b), (d) picture of the steep
418 bedding of Jurassic layers close to the southward thrust (see location on Fig. 4b).

419 Fig. 5 (a) Simplified geological map of the Hutubi He area (modified after XBGMR, 1978,
420 1993) with few structural measurements from field work. 'A' indicates location where Middle

Jurassic deposits directly and unconformity lie onto Carboniferous basement without Triassic or Lower Jurassic, (b) Geological cross-section along the Hutubi He constrained by field data, seismic profile (after Wang et al., 2005) and nearby drill wells W1 and W1'. Location of the section is indicated on Fig. 5a. Extension of the available seismic profile is indicated on the section.

Fig. 6 Examples of onlap structures of the Jurassic sediments over the Paleozoic basement units. (a) Picture and interpretation field sketch of the southern part of the Hutubi He (see location on Fig. 5a): note the overall southward onlap of the Jurassic sediments over the folded basement. To the north, a basement block is back thrusted over the sediments (see Fig. 5b), (b) Picture and interpretation field sketch of a small valley, west of the Hutubi He (see location on Fig. 5a): meso-scale basement relief covered by Jurassic sandstones as evidenced by onlaps over a steep inherited ~150 m high basement paleorelief (scarp). Basement rocks are deformed with a large inclined Paleozoic fold.

Fig. 7 Structural and sedimentological observations in the Wusu area. (a) Simplified geological map (modified after XBGMR, 1973) with few structural measurements. (b) Geological cross-section constrained by field data, seismic profile and drill well W2 (see Fig. 7a for location). (c) Picture and corresponding field sketch interpretation of the unconformable contact between Jurassic layers and the Carboniferous basement (see Fig. 7a for location).

Fig. 8 Sketch views of the paleogeographic evolution of the northern piedmont of Tian Shan during Early, Middle and Upper Jurassic/Cretaceous boundary. Main observations that constrain this study are localized on the drawings as: A for Fig. 3a; B for Fig. 4c (lower Jurassic sedimentary breccias); C for Fig. 6a (onlap covering of Paleozoic basement rocks by

444 Jurassic sandstones) and D for Figs. 3b and 3c (thick Kalaza Fm. breccias with angular
445 discordance at the base).